



Sonar 2021-2022 field experiment method development

A Case-Study of Seaweed Cultivation and biomass estimation using different sonar techniques and image recognizing networks

Authors: Romy Lansbergen, Hendrik de Villiers and Marnix Poelman

Wageningen University &
Research report C010/23

Sonar 2021-2022 field experiment method development

A Case-Study of Seaweed Cultivation and biomass estimation using different sonar techniques and image recognizing networks

Authors: Romy Lansbergen¹, Hendrik de Villiers² and Marnix Poelman¹

Wageningen Marine Research¹

Wageningen Food & Biobased Research²

This research project was carried out by Wageningen Marine Research, and Wageningen Food and Biobased Research. This report was funded by the WUR internal program KB34 Towards a Circular and Climate Neutral Society (2019-2022), project KB34-2C-4; title: Marine lower trophic food systems.

Wageningen Marine Research
Yerseke, March 2023

Wageningen Marine Research report C010/23

Keywords: seaweed, biomass estimation, sonar techniques, image recognizing networks

Client: Ministerie van Landbouw, Natuur en Voedselkwaliteit
Attn.: Directie SKI
P.O Box 2040
2500 EK, Den Haag

BAS code KB-34-007-004 1-2C-4

This report can be downloaded for free from <https://doi.org/10.18174/591184>
Wageningen Marine Research provides no printed copies of reports

Wageningen Marine Research is ISO 9001:2015 certified.

© Wageningen Marine Research

Wageningen Marine Research, an institute
within the legal entity Stichting Wageningen
Research (a foundation under Dutch private
law) represented by
Drs.ir. M.T. van Manen, Director Operations

KvK nr. 09098104,
WMR BTW nr. NL 8113.83.696.B16.
Code BIC/SWIFT address: RABONL2U
IBAN code: NL 73 RABO 0373599285

Wageningen Marine Research accepts no liability for consequential damage,
nor for damage resulting from applications of the results of work or other data
obtained from Wageningen Marine Research. Client indemnifies Wageningen
Marine Research from claims of third parties in connection with this
application. All rights reserved. No part of this publication may be reproduced
and / or published, photocopied or used in any other way without the written
permission of the publisher or author.

A_4_3_2 V32 (2021)

Contents

Summary	4
1 Introduction	5
1.1 General	5
1.2 Seaweed	5
1.3 Remote sensing techniques	6
1.4 Objectives	7
2 Materials and Methods	8
2.1 Study sites	8
2.2 Materials	9
2.2.1 DIDSON	9
2.2.2 Humminbird	10
2.3 Methodology	10
2.2.3 Sampling dates and conditions	10
2.2.4 Wet weight seaweed 2021	11
2.2.5 Image Preprocessing	11
2.2.6 Classical Vision Approach	11
2.2.7 Neural Network Approaches	12
2.2.8 Segmentation Metrics	20
3 Results	21
3.1 Sonar images (Humminbird 2021)	21
3.2 Sonar images (DIDSON in 2021)	22
3.2.1 Image Analysis	22
3.3 Sonar images (Humminbird 2022)	28
3.3.1 Classical Approach	29
3.3.2 Neural Network Approaches	30
3.3.3 Summary and conclusion	36
3.4 Seaweed biomass	38
4 Conclusions and recommendations	40
4.1 Limitations	40
4.2 Feasibility	40
4.3 Applicability	41
4.4 Recommendations	41
5 Quality Assurance	42
References	43
Justification	44

Summary

Seaweed is increasingly becoming a crop of interest in aquaculture. Seaweed has potential as a low trophic food source as no fresh water or fertiliser is needed for its growth. However, to start a profitable business in seaweed farming in the North Sea, space is required. Besides that, offshore seaweed farming is met with numerous technical challenges in this sometimes-turbulent environment. To monitor the crop farmers can make use of the latest technology in remote sensing. Potential remote sensing technologies, which could be used in seaweed farming, were identified in 2020. The use of the DIDSON sonar was thought in advance to make the most useful underwater images of the seaweed *Saccharina latissima* in a test farm in the Oosterschelde. Were in 2020 the first preliminary images were made with the DIDSON.

In 2021 the DIDSON was used to make images in the seaweed test farm, in combination with using Humminbird sonar (Helix 12, MSI/GPS G3N). In situ, it was found that handling the DIDSON while in a small boat was a difficult task. Because of movement of the sonar, it was difficult to make sharp images. The DIDSON again did not yield a lot of useful images. However fully convolutional neural network models for image recognition were tested using images from both years. The Humminbird fish finder was not successful in taking any images of seaweed in 2021, though the mussel lines in the same farm could be detected.

In 2022 the last sampling was done again using both sonars. This time using different settings, the Humminbird was able to detect the seaweed in the lines in the farm. The images that the Humminbird yielded had a better resolution and quality than those of the DIDSON from the previous years. This data could be used on further expanded neural networks. The images of the Humminbird were used in a classical approach for segmenting in the neural network and showed promise for future use. However the data had a lot of limitation and in follow up studies multiple lines should be measured using the Humminbird sonar. For the deep learning architecture, to further expand the neural network a larger test dataset is needed.

Besides the neural network, the biomass of the seaweed was also measured and samples were taken to the institute to measure length and surface area. However there didn't seem to be a clear correlation between seaweed length and biomass. To be able to estimate biomass from sonar images sufficient biomass measurements need to be made to determine the correlation, before accurate biomass predictions can be made using the segmentation in the neural network.

1 Introduction

In a previous study by Lubsch et al., (2020), the feasibility and use of a DIDSON Sonar was studied in relation to remote biomass estimation of sugar kelp (*Saccharina latissima*). That study was a first attempt, and had a high error margin. But the study provided some useful images, which were of interest for further research. Therefore in this study, we adapted some of the analysing methods and added a different type of sonar to continue and improve of the monitoring of seaweed with sonars. With an added addition of comparing the DIDSON sonar with a more modern fish finder sonar from the Humminbird series, and using an image recognising analysis in the form of a neural network, the feasibility of remotely estimating seaweed biomass and/or condition can be investigated.

1.1 General

The cultivation of seaweed is rapidly expanding, both increasing in biomass production as in spatial range. Most seaweed is cultivated in Asia. An increasing number of other countries now see the value and potential benefit in farming more low trophic marine species, and the promotion of seaweed as a “super food” has taken on its popularity in Europe. Therefore, seaweed farming is now upcoming in Europe. Since seaweed aquaculture is a new industry in Europe, there is a focus to innovate the processing and cultivation technologies used. At the moment the majority of the Dutch seaweed cultivation takes place in the Oosterschelde. However, the Dutch government has ambitions on expanding the seaweed cultivation offshore in the North Sea. The offshore cultivation can be in standalone cultures or in a multi-use setting in windmill parks. However, the North Sea is known for its rough weather conditions during the fall. For offshore cultivation to take place, a lot of technological challenges will have to be faced.

1.2 Seaweed

One of the main seaweed species cultivated in Europe is *Saccharina latissima*. *S. latissima* is a brown algae, also called sugar kelp or sea belt, and is considered a winter seaweed. It is seeded on horizontal cultivation lines in late autumn and harvested in late spring. It is therefore considered a winter species, unlike the other known seaweed species *Ulva lactuca* (sea lettuce) which is a summer species. *S. latissima* is considered a popular choice of cultivation due to its fast growth, biomass yield, and potential for commercial value (Azevedo et al. 2019).

1.3 Remote sensing techniques

For offshore farming of seaweed, remote sensing can be used to monitor the growth of the seaweed. There are several types of remote sensing with potential, such as ROVs, sonar and satellite imaging, however the logistics for monitoring the crops at sea is still an understudied field. The use of different types of sensors to monitor the crops at sea were investigated to assess their practical applicability and the pro's and con's for use for offshore seaweed farming (table 1).

The applicability of each sensor depends on what has to be measured. Many of the remote sensing tools can estimate distribution of macroalgae, and some can classify algae groups. The user friendliness and costs are also a choice, some of the data gathered needs to first be calibrated and analysed with software before an image can be used. Additionally, some of these tools are highly technical and costly. The types of sensors can range from remote sensing techniques using satellites to using soundwave-based sonar from onboard a ship. Additionally for seaweed biorefinery, the monitoring of biomass and seaweed condition is important, due to the high fresh biomass needed for processing. Knowing the biomass and condition of the seaweed will help choose the moment of harvest. This is important, because harvesting too early and the seaweed could have had more value if grown more, but too late and the seaweed could have gained biofouling organisms, decreasing the value of the seaweed. For the cultivation of seaweed in the North Sea, it is therefore important to have a method of monitoring the biomass and condition.

Table 1 Different types of remote sensing techniques possible for use on measuring seaweed and its pro's and con's.

Type sensor	Applicability (Pro's/con's)	Reference
Satellite imagery (hyper or multispectral)	Pro's: Large coverage, can be used in clear tropical waters. Large data sets available, open source. Con's: course resolution, trouble in murky waters, time of images does not take tides into account. Weather conditions can impact quality.	Bennion et al.,(2019)
Aerial imagery (Drones or planes)	Pro's: Effective for area distribution, high resolution, multiple spectra can be gathered which can aid in classification of species. Con's: Weather dependent, light based, so murky/deep waters can effect quality. Time consuming (flying drones, then analysis data.	Bennion, (2018) Bennion et al.,(2019)
Underwater imagery (AUV)	Pro's: high resolution, close up view Con's: slow processing of data, only applicable on small scale and murky waters effect quality, need a boat to steer underwater vehicle, or	Bennion, (2018) Bennion et al.,(2019)
LiDAR (light detection and ranging)	Pro's: large coverage, open source data, quantitative data. Con's: Turbidity impacts quality, Tides effect quality, data availability limited per region.	Bennion et al.,(2019)
Sonar (sound navigation and ranging)	<u>Multi-beam echo sounder (DIDSON)</u> Pro's: data is quantitative, which can later be used in models for biomass. multiple beams make picture Con's: harmonisation of different backscatter information difficult to manage. Calibration difficult. Needs to hang still, movement causes less quality picture. Expensive, specialised technology. Ineffective in shallow waters <2 meter	Bennion et al., (2017) Bennion et al., (2019) Burggraaf, pers commun.
	<u>Side scan fishfinder (Humming bird):</u> Pro's: the hummingbird can be attached to the underside of a small boat, by sailing slowly you will get a stable picture. Highly visual image. Cheap, can buy in the commercial market Con's: Only using one beam per ping, so you will have to move it through the water to get a line to form an image. no extra data, so no modelling possible.	

1.4 Objectives

The aim of this study is to compare different types of remote sensing techniques and the use of image recognition to create a truly remote analysis of seaweed biomass. This is a method developing study whereby the limitation and applicability of two different types of sonar were compared and evaluated. Additionally, a machine learning technique was applied to the sonar images to evaluate if it was possible to make a model, which can recognise seaweed and predict biomass. At the end of this report the results of the different types of sonar and the machine learning results are presented.

2 Materials and Methods

2.1 Study sites

The measurements were conducted in the Oosterschelde in two locations in 2021 and 2022 (Fig 1), both on the same seaweed species. The first year 2021, sonars were tested on a single line of seaweed cultivated at a seaweed test location in the Matten haven near the Island of Neeltje Jans. The seaweed test location is owned and operated by Stichting Zeeschelp B.V. The measured seaweed line was 21 meter long, and sonar images were gathered at this location twice, once in March and once just before harvest in June. The cultivation line in question was hanging in a suspension plot for the cultivation of the blue mussels (*Mytilus edulis*). The suspension lines in a north/southern direction. In May 2022 the sonars were tested at a second location, which was Schelphoek. Sonars were tested on multiple lines at the seaweed farm from the Dutch Seaweed Groep (DSG). DSG has multiple lines of different seaweed species in this location. Image capture with both sonars was preformed on seaweed lines with sugar kelp (*Saccharina latissima*) just before harvest.

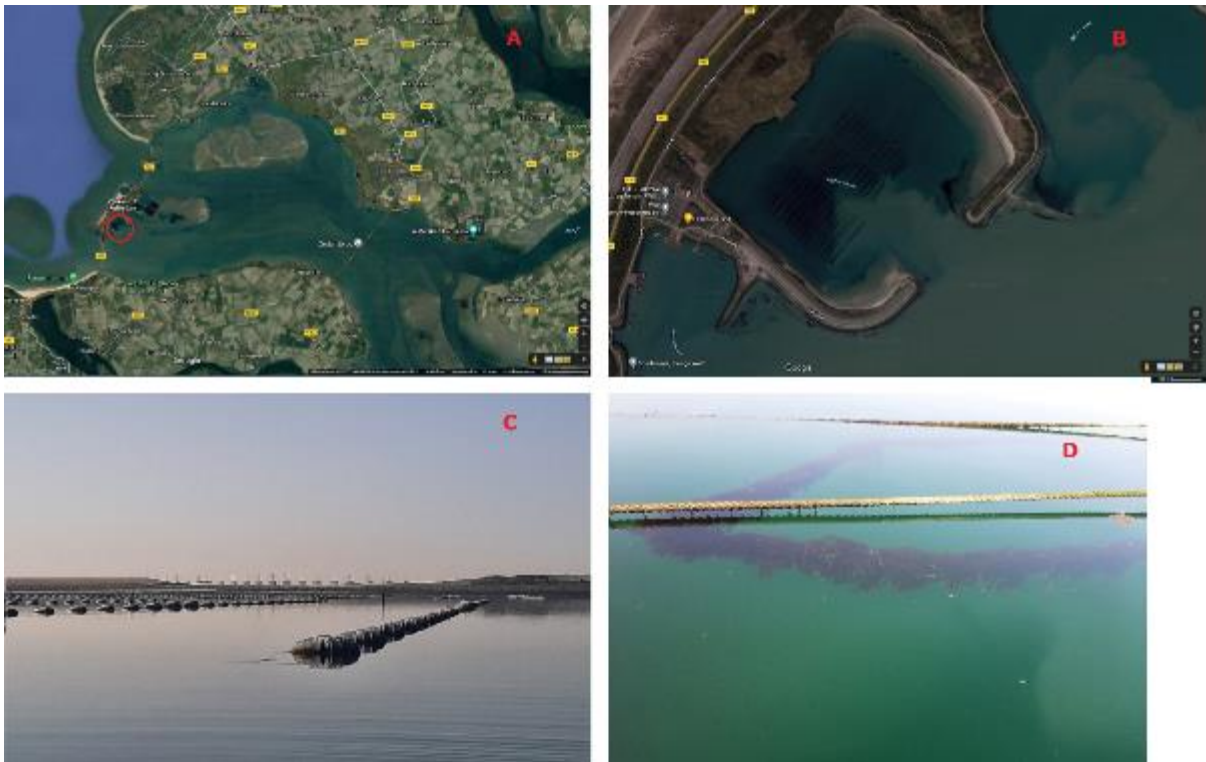


Figure 1 Overview of experimental site 2021

A: Aerial shot of the Oosterschelde circled is the Matten haven at the Neeltje Jans island(google maps, 2021).

B: Zoomed in areal footage of the Matten haven, you can see the mussel suspension culture (google maps, 2021). C: Photo of the mussel suspension culture at the matter haven (photo: R. Lansbergen, 2021).

D: Photo of the seaweed line (01-03-2021) hanging between-the mussel suspension lines (photo R. Lansbergen, 2021).

2.2 Materials

Two types of sonar were used to make images of a single line of seaweed. The DIDSON handheld multibeam sonar and the under the boat fastened Humminbird single beam sonar.

2.2.1 DIDSON

The first sonar used was a DIDSON (DIDSON-sonar, Diver-held 100m; Sound Metrics Corp., Bellevue, WA, USA, fig 2.), this is the same sonar that was used in the preliminary study of 2020. The DIDSON sonar is a multi-beam sonar that can be submerged and manoeuvred by hand. The sonar was attached to the end of a 3 meter long stainless steel pole ($\varnothing = 40$ mm), as was done previously in 2020. The pole was attached to a metal tube guard, which was placed on the inflatable tube of the RIB. The DIDSON was both mounted at a 90° angle and “normally” (straight), after which the sonar was submerged and manoeuvred using the pole as a handle (fig, 2). The DIDSON was connected to a computer by a cable, transferring data and power. Additionally, a safety cord was tied to the DIDSON to prevent loss. The sonar specifications were set as follows in table 2.



Figure 2 Hand held DIDSON sonar device (Photo, H. Verdaat, 2021).

Table 2 Parameters of the DIDSON sonar used during field testing in the Oosterschelde

Parameter	Value and unit
Identification frequency	1.8 MHz
Sound speed	1457 m/s
Beams	96
Sample rate	37.3 KHz
Rcv Gain	40 dB
A2D-PS	24-21 C

Analysis of the sonar recordings was conducted with the DIDSON-Sonar Control and Display Software Version 5.26.40. Snapshots of the sonar images were made when the seaweed was seen most clearly on the laptop. In addition to the snapshot when the RIB was motionless next to the seaweed line, a recording was also taken when the RIB did a the sweep alongside the seaweed line.

2.2.2 Humminbird

The Humminbird used (Helix 12, MSI/GPS G3N, fig 3) is a dual beam side and down scanning sonar which has a transducer which is placed under a boat. The separate display screen is mounted on the console so a live image can be seen. The Reef master software was used for first analysis and extraction of the images.



Figure 3 Humminbird visual console on the RIB Scheurrak.

2.3 Methodology

2.2.3 Sampling dates and conditions

Table 3. Sampling dates and conditions experimental work

Date	Tide	Wind (bft)	Remarks	Location
31-03-2021	Low	0	Wind still conditions, weighting of the seaweed done by WPR	Matten haven Neeltje Jans
01-06-2021	High	2	Trouble handling the DIDSON sonar	Matten haven Neeltje Jans
04-06-2021	N/A	1	Harvesting of total line + sample taken of 15 cm piece of line.	Matten haven Neeltje Jans
12-05-2022	Up -coming	2	Dutch seaweed group, was harvesting at the moment of sampling. Loss of DIDSON data.	Schelphoek DSG location

2.2.4 Wet weight seaweed 2021

The seaweed which was cultivated in 2021 was on a 21m single line and weighted 4,6 kg before seeding. The seaweed line was suspended between the mussel suspension lines. The seaweed cultivation line was weighed twice, both on the same day as the sonar measurement were taken. To weigh the cultivation line, the line was detached from the mussel hanging cultures it was placed in between and tied to the back of the RIB, the line was dragged slowly to a small platform. The dragging removed some of the loose seaweed leaves and other fouling. On the platform the line was let to drain most of the water before placed in a fishing box with some holes in the bottom to allow for water drainage (fig 4). The fishing box was placed on the scale and measured. The weight of the fishing box and the weight of empty cultivation line was subtracted from the total to allow for only seaweed wet weight. Seaweed was removed from the water only for a maximum of 10 minutes to avoid damage to the seaweed. The seaweed cultivation line was provided by Stichting de Zeeschelp B.V.



Figure 4 Seaweed on line in two fishing boxes, ready to be weighed for fresh weight (photo R. Lansbergen, 2021).

The seaweed lines from the Schelphoek (2022 data) were from the DSG and were unfortunately not weighted. The length and surface area of the seaweed was determined by taking photographs of the seaweed pieces and then using the image analysing software ImageJ. 10 pieces of the largest pieces of seaweed were taken back to lab to be individually weighted for wetweight and dried in a stove for 24 hours at 80°C for dry weight.

Using the surface area (SA) of the seaweed, a relative biomass could be approximated, if there is a correlation between the variables. By looking at the SA data and the weight (wet/dry), the R^2 can be calculated to see if there is a correlation between the SA or length and the biomass of the seaweed. If the sonar can determine either length or SA, the calculated results of the sonar measurement can then be compared with the wet weight of the cultivation line, to estimate biomass.

2.2.5 Image Preprocessing

For the data from the DIDSON device, DIDSON's own software was used to explore and preprocess data, as well as exporting images. For the Humminbird device, both 2021 and 2022 data were explored using the ReefMaster application. However, 2022 Humminbird data was preprocessed and exported using the Python library PyHum. This package allows for the complete export of a sonar scan to a format that can be imported directly into Python's scientific computation facilities (for example NumPy).

2.2.6 Classical Vision Approach

For the Humminbird 2022 data, a classical computer vision approach was explored to test the difficulty of the segmentation problem on this data. In addition, the approach was used to help label the data for use during neural network training. This is also the approach's main envisioned utility in future.

This approach consists of four main steps:

1. Normalization of the image between 0 and 1.
2. Denoising using a Gaussian kernel with standard deviation of 1.
3. Thresholding the denoised image such that regions with intensities greater than 0.45 are treated as seaweed candidates. Close to the top (row number less than 55), this threshold is

raised to 0.5, because it was found that spurious detections tend to occur here at lower thresholds.

4. Continuous pixel regions are identified, and then are eliminated subject to a set of rules:
 - a. Is the central row of the region in the first 50 or last 50 pixels? Then this is likely the top or seabed, and the region is dropped.
 - b. Is the region area less than 5000 pixels squared? Then it is likely a small spurious detection, and the region is dropped.

2.2.7 Neural Network Approaches

One goal of the project is to remove the need for human intervention during the calculation of seaweed biomass. Towards a fully automated pipeline (a sequence of operations transforming provided inputs to desired outputs), we first replace the image binarization process with a potentially fully automated approach based on Fully Convolutional Neural Networks (FCNs) / U-Net (Ronneberger et al. 2015). Specifically, these networks will be used to identify which pixels in an image contain seaweed of interest, and those that do not. This is known as an image segmentation task. Such models employ convolutions (**Figure 5**) in order to make decisions.



Figure 5. The emboss operation, an example of a convolution operation. Reproduced from Apple inc.(2016)

In order to train and test models, data are necessary. In 2021, it was found that, for the DIDSON data, there was not enough data to build a suitable training and test set. Therefore, the previous DIDSON images from the 2020 study by Lubsch et al. (2020) were used. In the 2020 and 2021 data, 16 still images were extracted as subjects for earlier analysis and as examples. This was enough to develop a workflow for automating the image binarization process to an extent. So, while a system based on these images was not necessarily expected to be successful, the system could be reused when more data are available or captured at a later date higher in quality, but also limited in quantity. The reason for the increase in quality is currently unknown (it is understood that the captain adjusted the settings on the device), and this should be subject to further investigation. This however allowed the testing of more complex U-Nets (Ronneberger et al. 2015) as part of the automated workflow, which enabled the neural network models to learn finer grained segmentation behaviours. FCNs (of which U-Nets are a subtype) are an elegant means of performing image segmentation. They also tend to require less training data than other neural network-based methods, which makes them particularly suitable to the present situation. They are based on repeated application of the widely used convolution operator to images, tuning individual convolution operators until the effect of the entire set of convolutions yields some useful operation.

An example of a single convolution operation in action can be given by the emboss effect. The effect of the emboss operator is to detect edges going in a certain direction. The entire operation can be characterized by a 3x3 matrix of numbers known as a kernel or filter (Figure 6).

-2	-2	0
-2	6	0
0	0	0

Figure 6 Matrix defining the emboss convolution (known as the kernel or filter). Reproduced from Apple Inc. (2016)

Convolutions work by sliding this matrix over the entire input image (Figure 7), and at each position, doing the same calculations. Corresponding numbers in the image and kernel are multiplied, and the resulting sum is output to the output image.

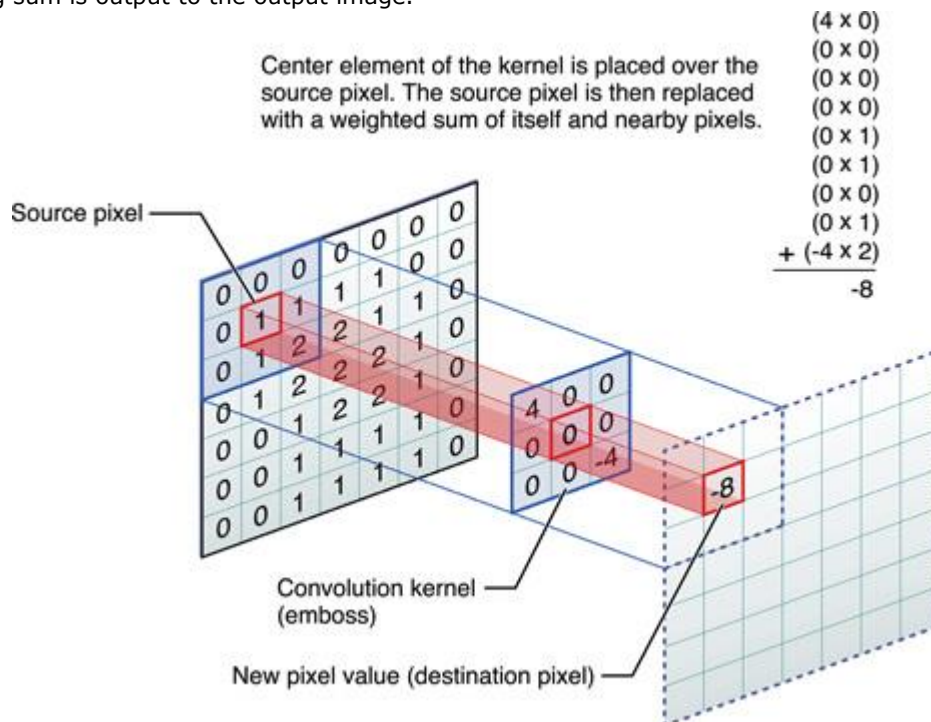


Figure 7 Functioning of the convolution operation. Reproduced from Apple Inc. (2016)

FCNs work by combining many convolutions operating in parallel and in series. Each convolution learns to do some basic operation like detecting a certain kind of edge in the image. The deeper one goes into the network of convolutions, the more abstract the convolution's apparent function may become. Finally, it is hoped that the combined operation of these convolutions can be steered towards the functionality that the user wants, such as detecting the location of seaweed. In practice, one may need to try a number of network architectures (roughly speaking arrangement and connections of the convolutions and other mathematical components) before a suitable one can be found. In this work, five different neural network architectures were tested on the 2021 dataset as to their suitability for binarization of the sonar images of seaweed. A further two architectures were tested on the 2022 dataset. These architectures are described by (Fig Figure 8) through (Fig Figure 14).

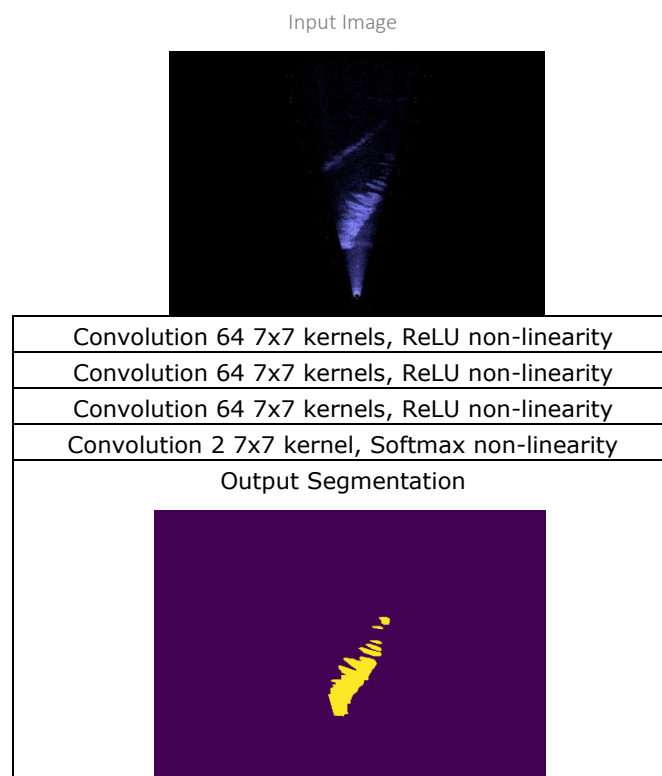


Figure 8 Architecture of the shallowest neural network tested. Information flows from top to bottom through each layer of the network, starting with the input image and producing the output segmentation at the end. This architecture was applied to the 2020-2021 DIDSON data.

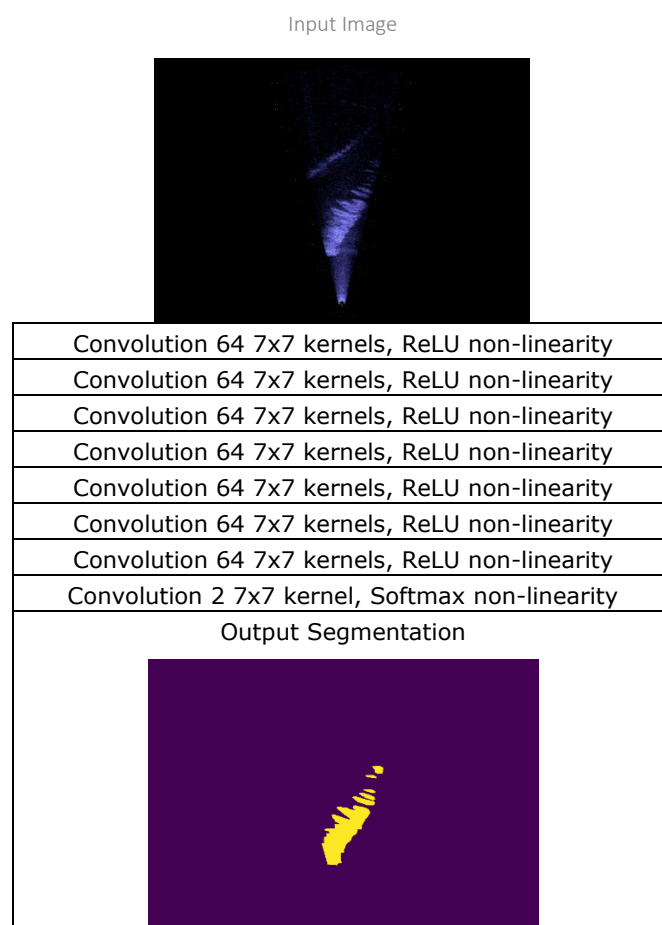


Figure 9 A medium-depth variant of the initial network architecture. This architecture was applied to the 2020-2021 DIDSON data.

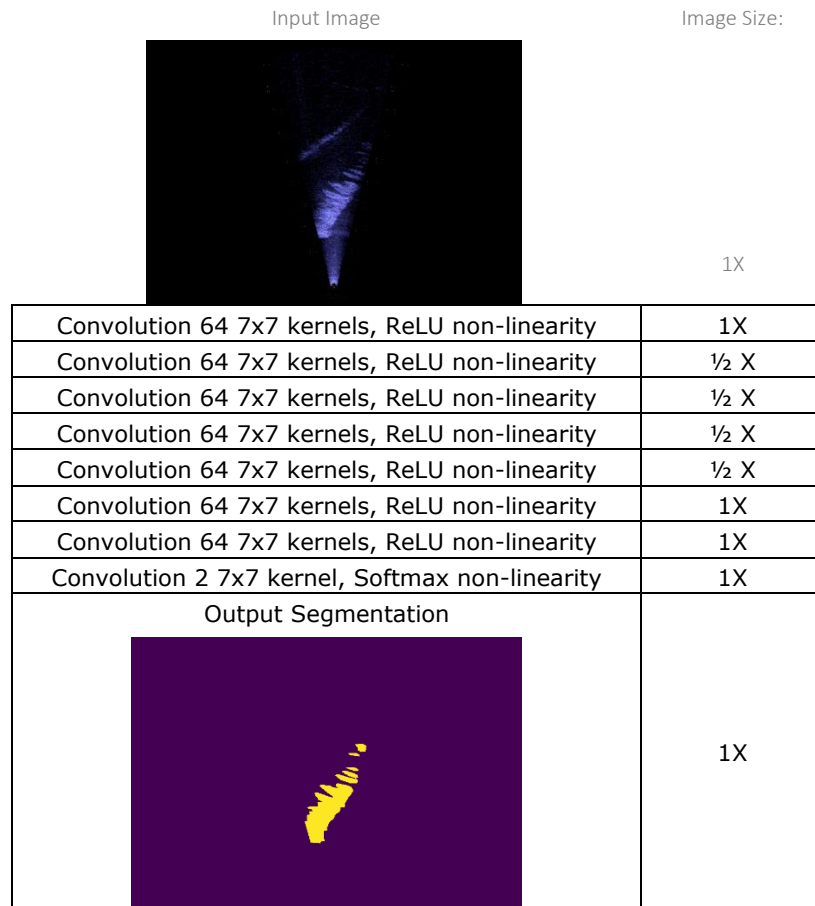


Figure 10 Medium depth variant with one level of pooling/unpooling. The image size changes as it passes through the network, shrinking by a factor of 2 when pooling occurs, and increasing by a factor of 2 when unpooling occurs. This architecture was applied to the 2020-2021 DIDSON data.

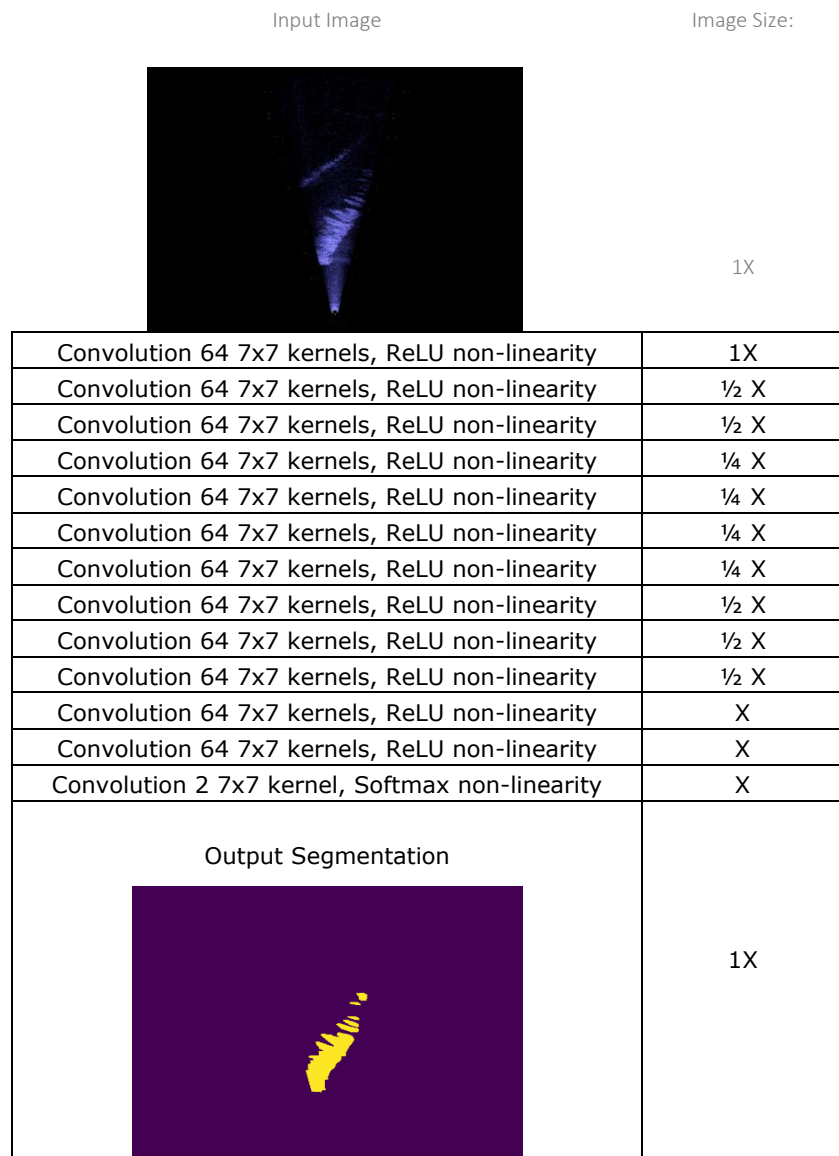


Figure 11 Deep variant with two levels of pooling/unpooling. The image size changes as it passes through the network, shrinking by a factor of 2 when pooling occurs, and increasing by a factor of 2 when unpooling occurs. This architecture was applied to the 2020-2021 DIDSON data.

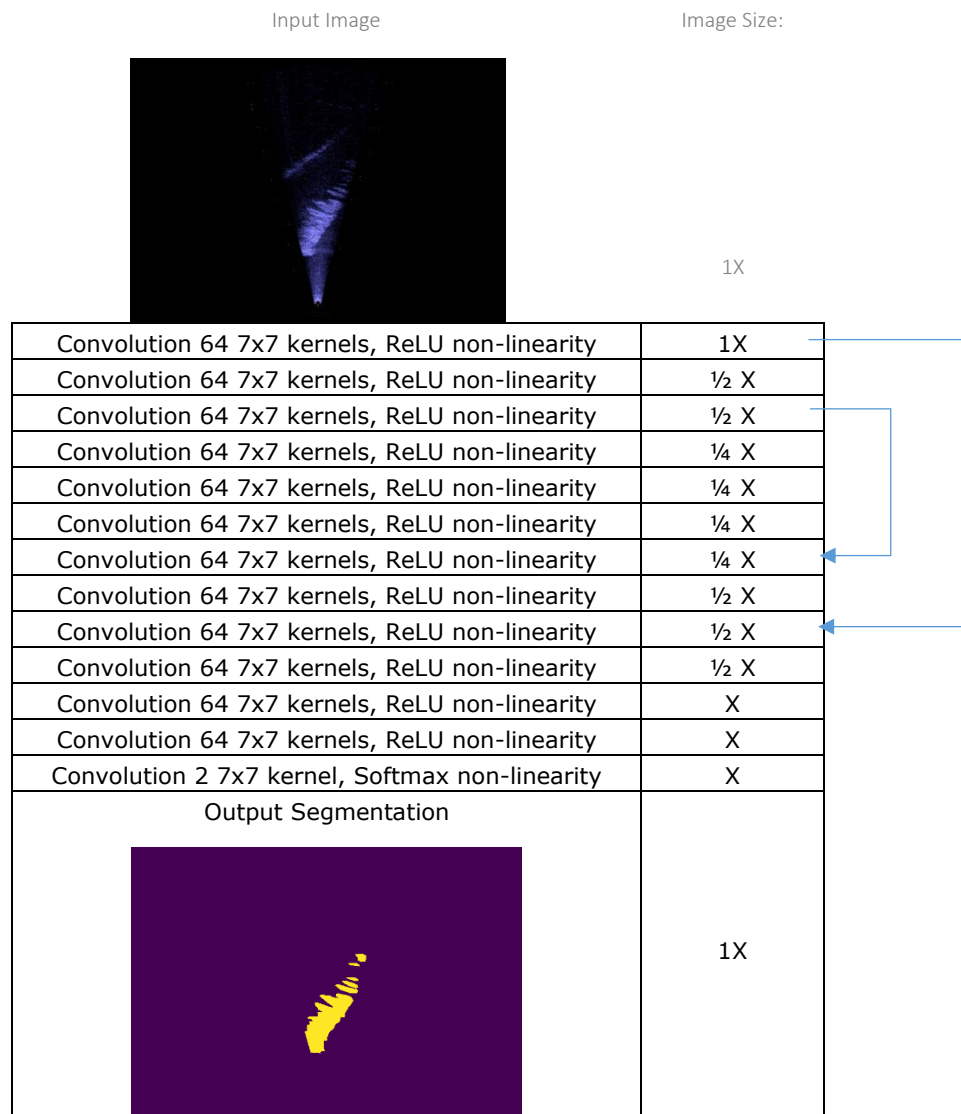


Figure 12 Deep variant with two added skip connections. High-resolution information is passed forward to deeper layers as indicated by the arrows. This architecture was applied to the 2020-2021 DIDSON data.

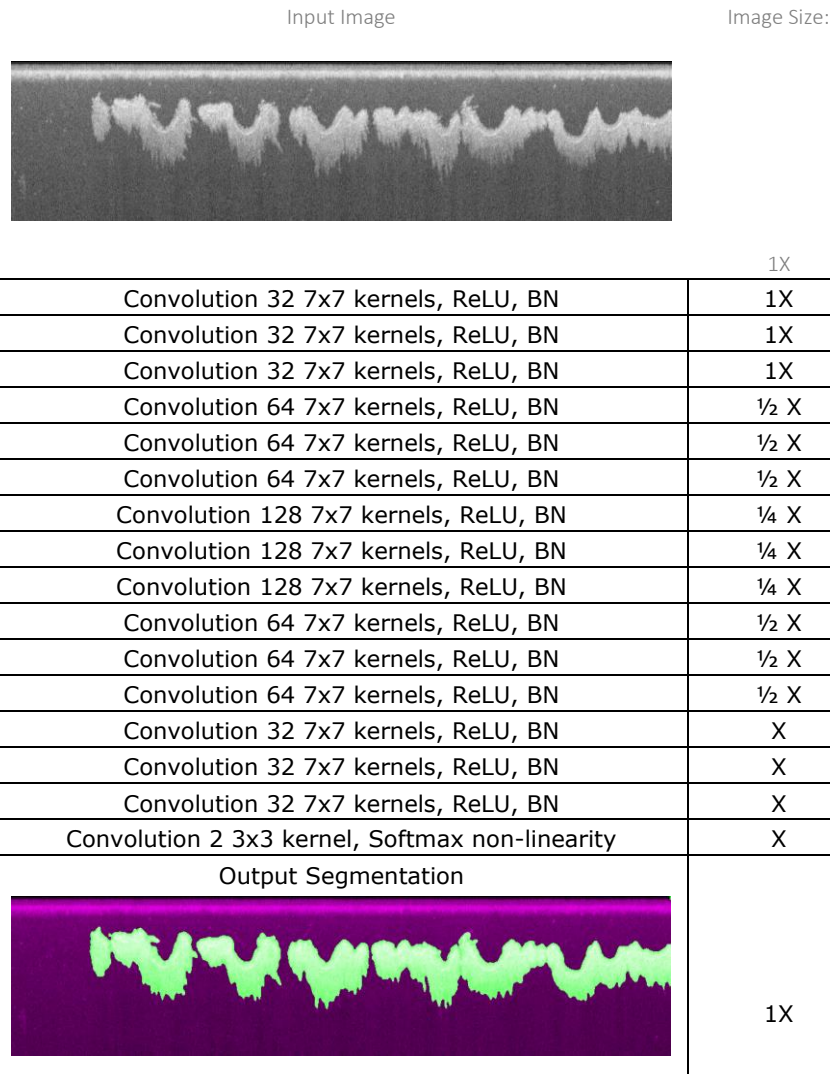
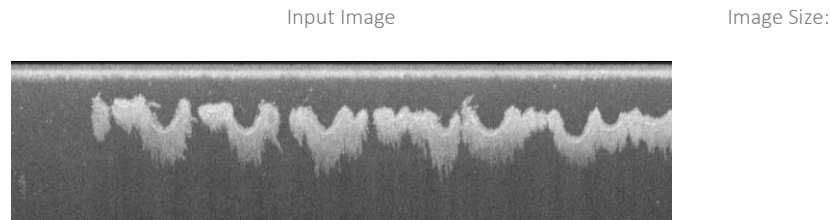


Figure 13 Deeper variant (Deep3) with three added skip connections. Each level contains three instead of two convolutions. Batch normalization (BN) is added to improve performance. High-resolution information is passed forward to deeper layers as indicated by the arrows. This architecture was applied to the 2022 Humminbird data.



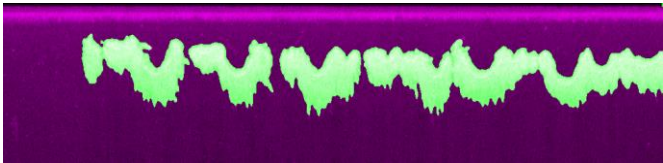
		1X
Convolution 32 7x7 kernels, ReLU, BN	1X	
Convolution 32 7x7 kernels, ReLU, BN	1X	
Convolution 32 7x7 kernels, ReLU, BN	1X	
Convolution 64 7x7 kernels, ReLU, BN	1/2 X	
Convolution 64 7x7 kernels, ReLU, BN	1/2 X	
Convolution 64 7x7 kernels, ReLU, BN	1/2 X	
Convolution 128 7x7 kernels, ReLU, BN	1/4 X	
Convolution 128 7x7 kernels, ReLU, BN	1/4 X	
Convolution 128 7x7 kernels, ReLU, BN	1/4 X	
Convolution 256 7x7 kernels, ReLU, BN	1/8 X	
Convolution 256 7x7 kernels, ReLU, BN	1/8 X	
Convolution 256 7x7 kernels, ReLU, BN	1/8 X	
Convolution 512 7x7 kernels, ReLU, BN	1/16 X	
Convolution 512 7x7 kernels, ReLU, BN	1/16 X	
Convolution 512 7x7 kernels, ReLU, BN	1/16 X	
Convolution 256 7x7 kernels, ReLU, BN	1/8 X	
Convolution 256 7x7 kernels, ReLU, BN	1/8 X	
Convolution 256 7x7 kernels, ReLU, BN	1/8 X	
Convolution 128 7x7 kernels, ReLU, BN	1/4 X	
Convolution 128 7x7 kernels, ReLU, BN	1/4 X	
Convolution 128 7x7 kernels, ReLU, BN	1/4 X	
Convolution 64 7x7 kernels, ReLU, BN	1/2 X	
Convolution 64 7x7 kernels, ReLU, BN	1/2 X	
Convolution 64 7x7 kernels, ReLU, BN	1/2 X	
Convolution 32 7x7 kernels, ReLU, BN	X	
Convolution 32 7x7 kernels, ReLU, BN	X	
Convolution 32 7x7 kernels, ReLU, BN	X	
Convolution 2 3x3 kernel, Softmax non-linearity	X	
<div style="display: flex; align-items: center;"> <div style="text-align: center; flex: 1;"> <p>Output Segmentation</p>  </div> <div style="text-align: center; flex: 1;"> <p>1X</p> </div> </div>		

Figure 14 Deepest variant (Deep5) with five added skip connections. Each level contains three instead of two convolutions. Batch normalization (BN) is added to improve performance. High-resolution information is passed forward to deeper layers as indicated by the arrows. This architecture was applied to the 2022 Humminbird data.

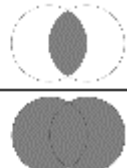
The neural network architectures explored three design themes:

- Network depth: Deeper networks (networks with more layers) are generally able to perform more complex operations. However, because of this extra complexity, such networks may become “too smart” and overfit (simply remember the training data instead of “understanding” it).
- Pooling/unpooling: Pooling and unpooling shrinks and grows the image as it is being processed by the network. When shrunk, operations on an image cover larger areas of the original image, and so the network is able to gather more information from the context. Generally this comes at the cost of high-resolution information passing through the network, meaning resulting segmentations can become less sharp.
- Skip connections: Pooled stages can have difficulty passing high-resolution information that can be essential for obtaining sharp segmentations. Skip connections pass such information forward in the network, bypassing the pooled stages, making the information available for the later stages in the network. Skip connections can help to obtain a sharper segmentation than an similar network without such connections.

To further conserve data, a kind of Leave One Out validation was employed during testing. When an image is tested, a model is first built using all the other images, and that model then applied to the test image. This is a slow process, however it maximizes the amount of images available during training (15 out of 16 in 2020/2021 data). However, note that we only tested images that contained some of the seaweed of interest, which occurred in seven out of 15 images of 2020/2021 data.

2.2.8 Segmentation Metrics

For the 2022 Humminbird data, primarily the Intersection over Union (IoU) (Shanmugamani 2018) was used to express the overlapping region (intersection) between a class in the prediction and ground truth as a percentage of their merged region (union). If the overlap between the areas is perfect, then the result is 1 (or 100%). If there is no overlap, the result is 0 (or 0%).

$$\text{IoU} = \frac{\text{Area of Overlap}}{\text{Area of Union}}$$


3 Results

3.1 Sonar images (Humminbird 2021)

By using the ReefMaster software, the mussel cultivation ropes on either side of the seaweed line could be seen (Fig 15). However, the seaweed line itself is only barely visible and the seaweed cannot be seen at all (Fig 15). It seems that the seaweed does not reflect the sonar beam from the Humminbird.

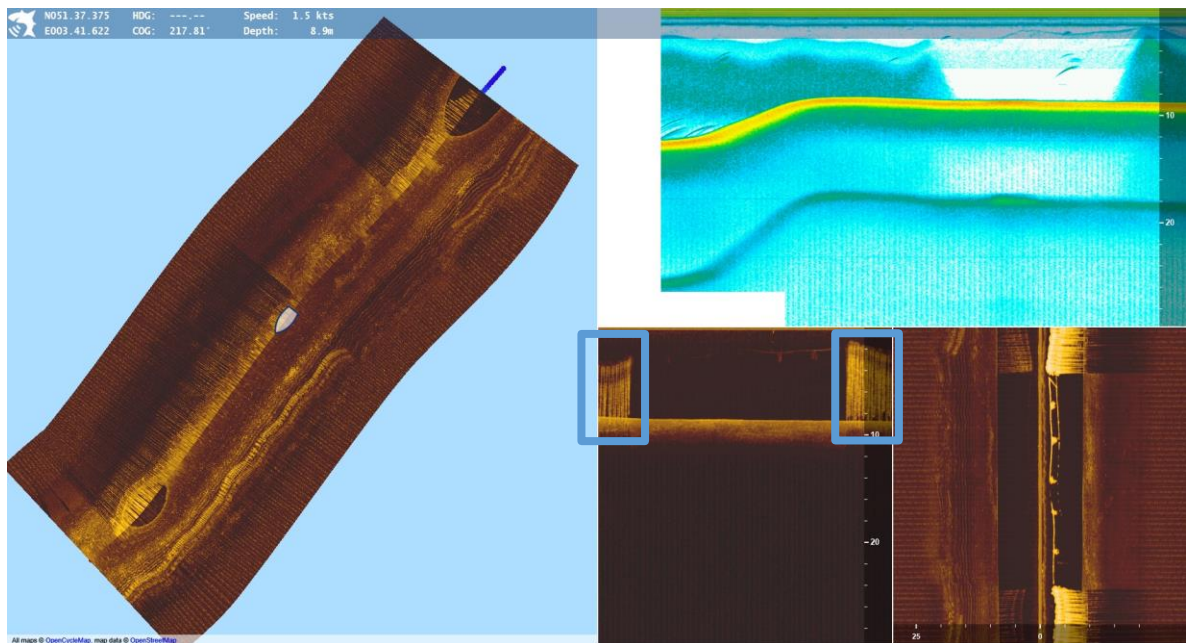


Figure 15 Reef master image of the Humming bird track. The gap can be seen in the lower central picture where the seaweed is but is not visible on the sonar. Mussel cultivation ropes (narrow loops going up and down) are marked in green rectangles in the central lower plot. Note the seaweed line is barely visible stretching between the two rectangles.

3.2 Sonar images (DIDSON in 2021)

The use of the DIDSON sonar resulted in about 30 images from the 2021 survey. However, it turned out that most of the images were not usable for further analysis due to angle, resolution or just no seaweed can be detected. In combination with the images taken in the previous survey only 7 images could be selected which were usable for the image analysis.

3.2.1 Image Analysis

Experiments began by considering the shallow network (**Figure 8**) and applying Leave One Out validation to the seven DIDSON images that contained some seaweed of interest (**Figure 16**). In the images the most of the bright regions are coloured red and these regions are considered by the network to be likely regions containing the seaweed of interest. This behaviour can be explained by considering the fact that such a shallow network has a very limited image context with which it needs to make decisions. Without being able to check the larger context, it is not unreasonable for the network to learn "bright regions are probably seaweed".

Towards improving this situation, a network of medium depth (**Figure 9**) was considered with corresponding output (**Figure 17**). The added layers contributed both the context the network can process and the complexity of the decision processes it can learn. The added depth improved results, with certain incorrectly highlighted regions from the previous case being less highlighted.

To further investigate increasing the context available to the network when making decisions, we introduced pooling and unpooling (**Figure 10**) into the preceding network producing a new set of output images (**Figure 18**). In most test images, the results were similar, except the network with pooling tends to prefer regions where the image didn't change as much. It was also particularly noticeable that two of the test images showed failure where most of the region was predicted as seaweed. These also are input images where there was significantly more background noise present than in most of the dataset, and the prediction failure was probably attributable to this.

To evaluate whether added depth may have helped the network, a more complex architecture was investigated (**Figure 11**) resulting in new outputs (**Figure 19**). The output of the network appeared worse. In particular, it was noticed that the network output was slow-changing. This could have been because high resolution information was getting lost as more pooling was applied.

In order to preserve high resolution information for use in the later parts of the network, two skip connections were added (**Figure 12**). These skip connections carry information forward in the network as is, making it available for later stages. This is especially useful for making detailed shape information available in later prediction stages of the neural network. The network's ability to follow the outlines of objects improved over the preceding case (**Figure 20**). Furthermore, the network was better at preferring the seaweed of interest over other objects, but there were still many false positives. In particular, those images containing heightened background noise were still poorly treated.

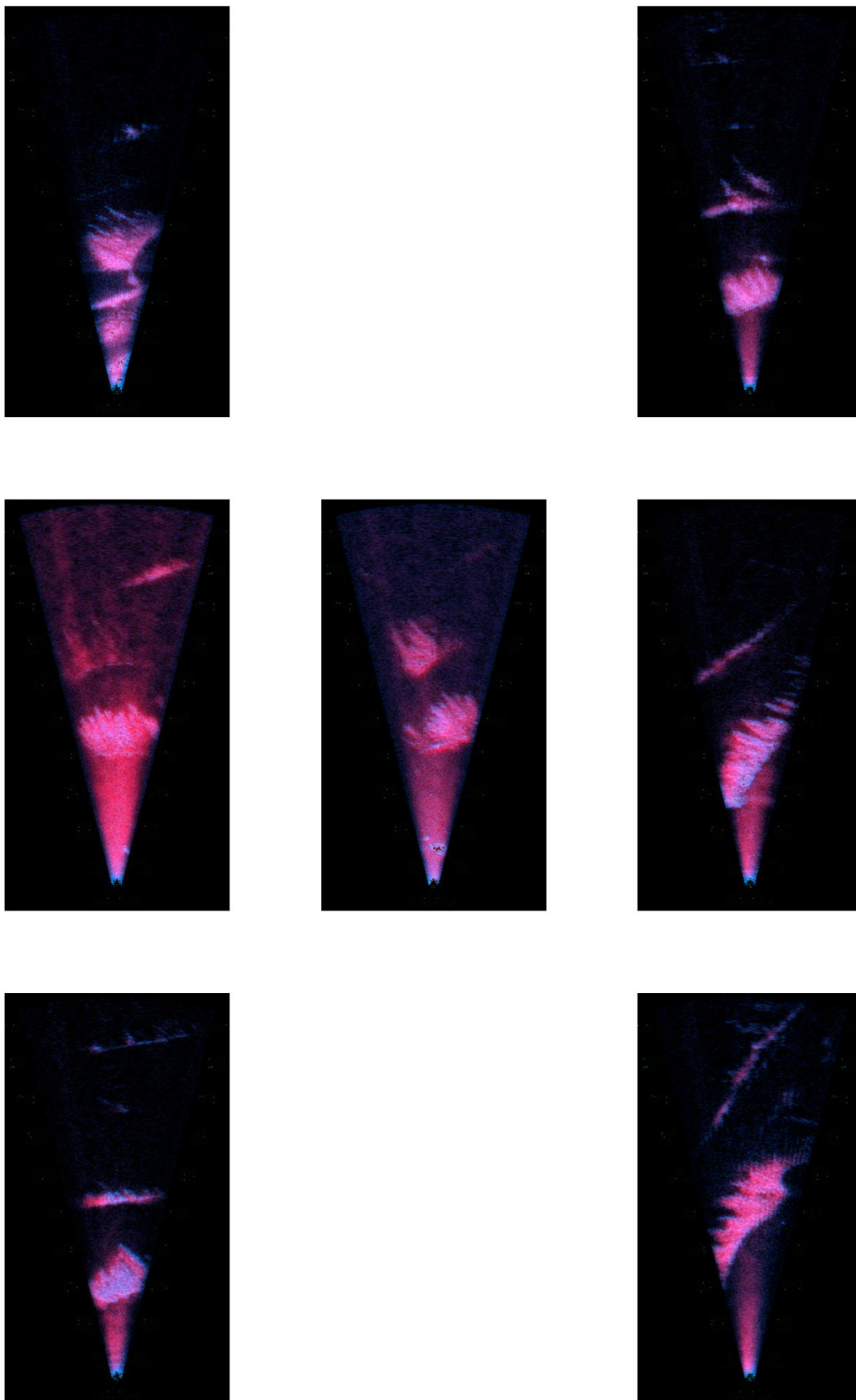


Figure 16 Output of shallowest network superimposed on the input.

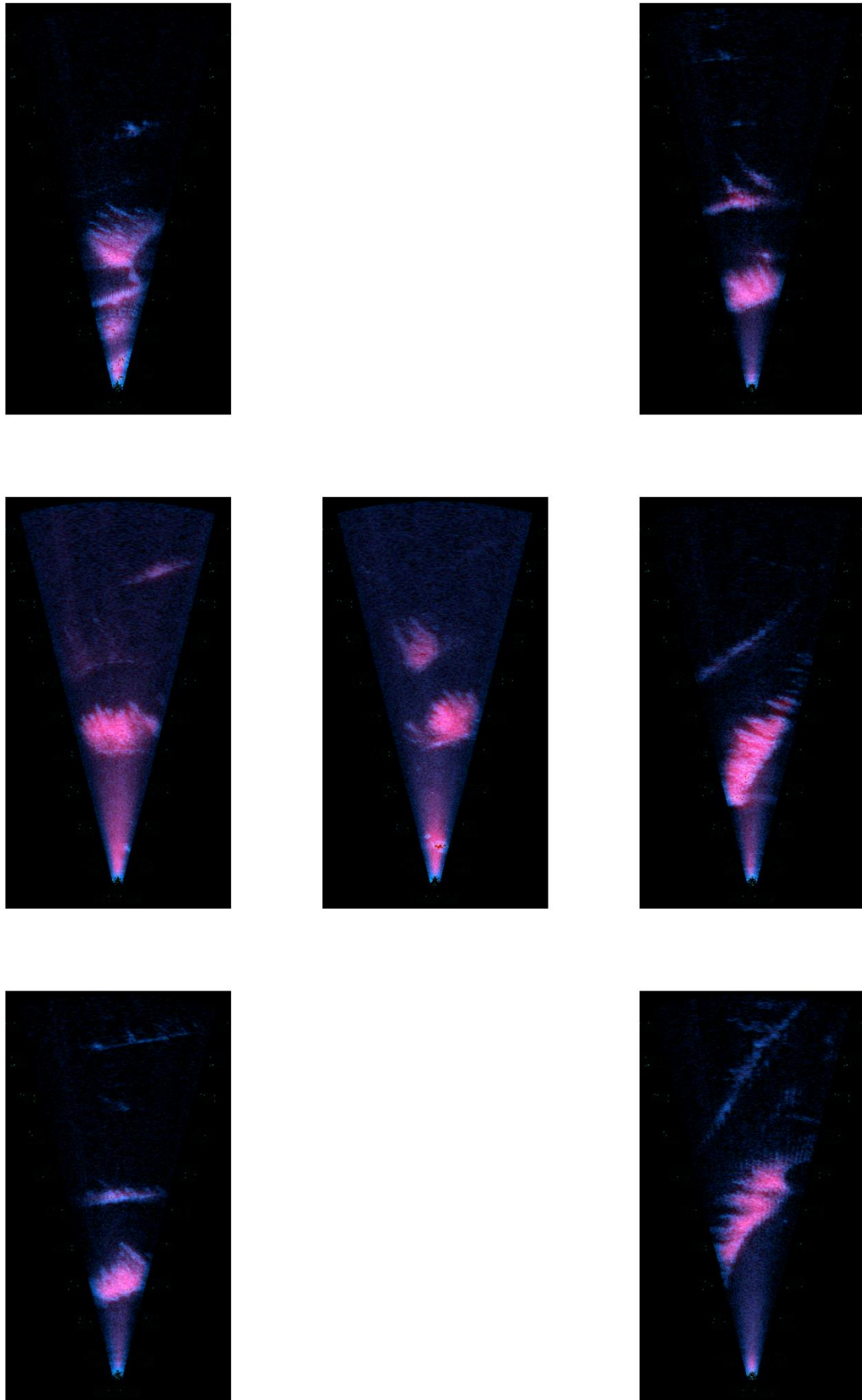


Figure 17 Output of medium depth network (without pooling) superimposed on the input.

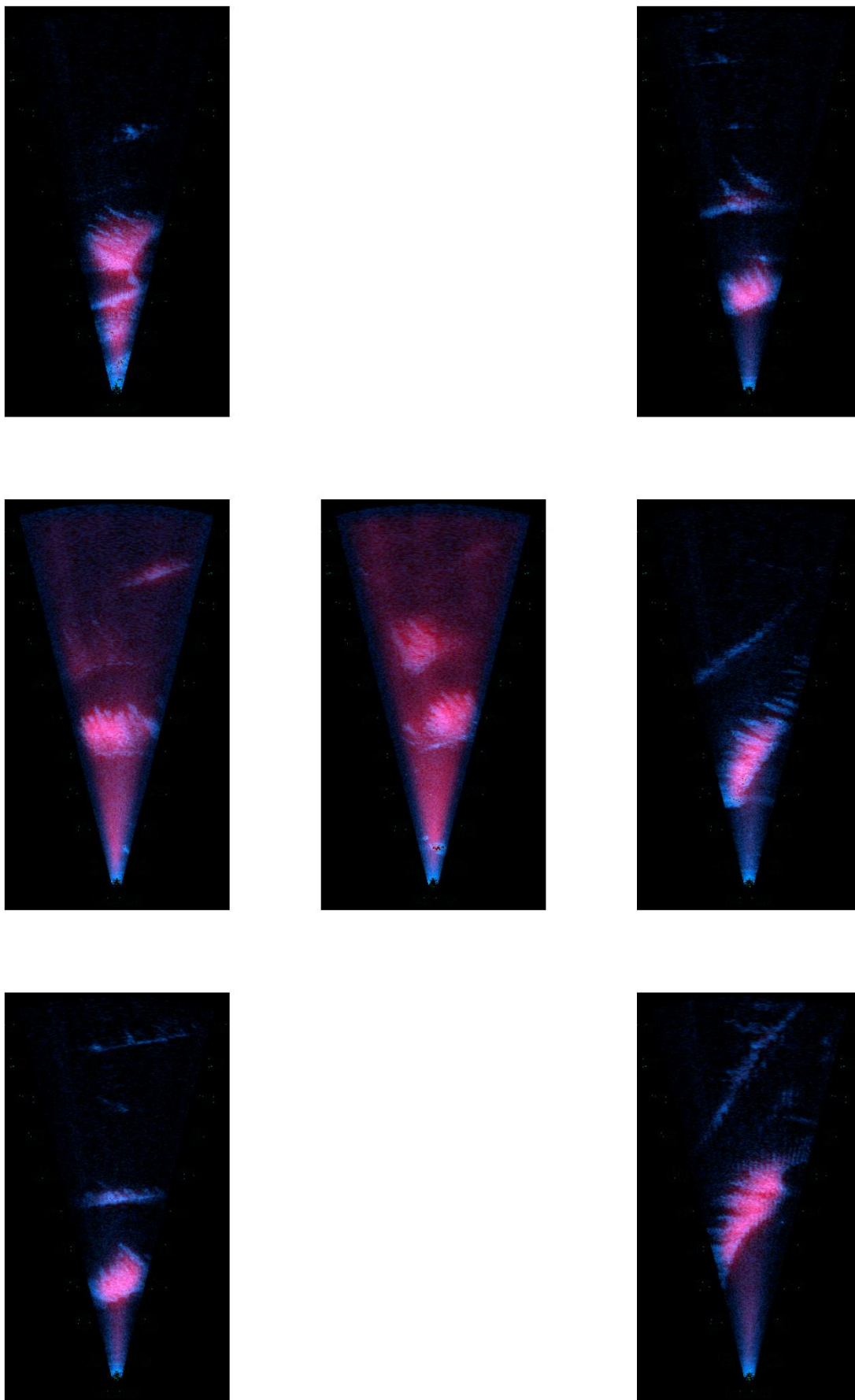


Figure 18 Output of medium depth network (with pooling) superimposed on the input.

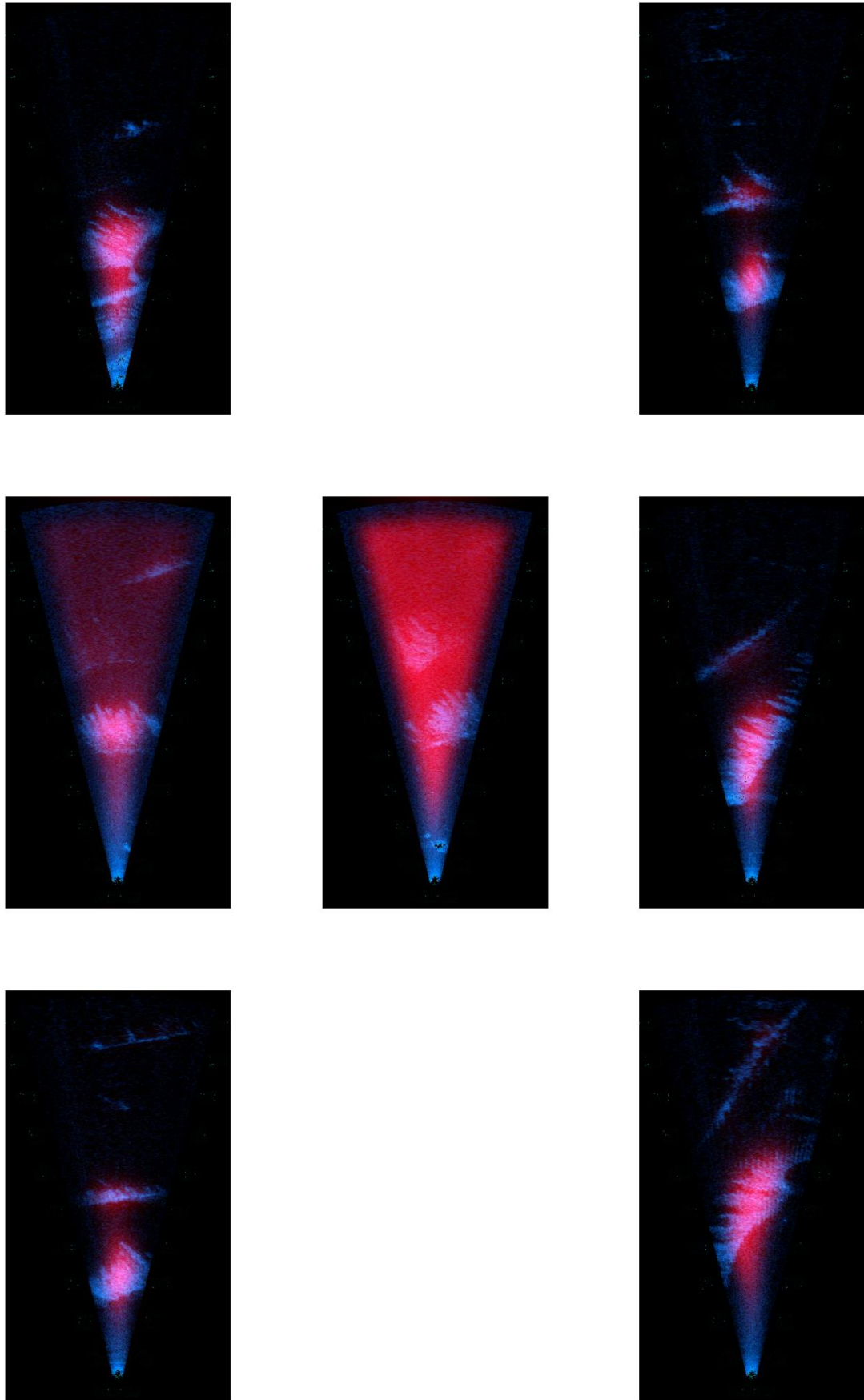


Figure 19 Output of deepest network (without skip connections) superimposed on the input.

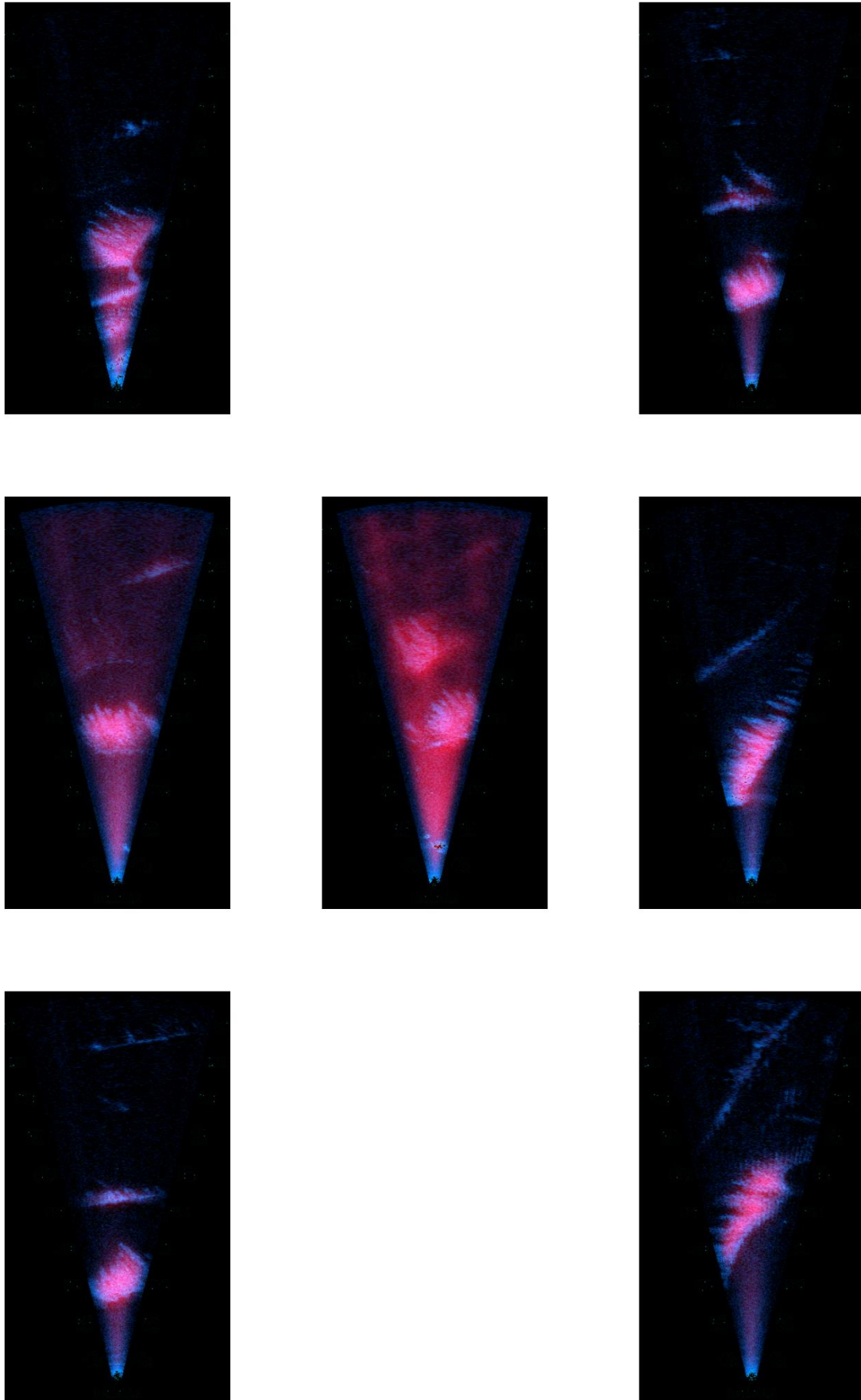


Figure 20 Output of deepest network (with skip connections) superimposed on the input.

3.3 Sonar images (Humminbird 2022)

Images obtained from the Humminbird in 2022 contrasted sharply with those obtained in 2021. While certain challenges remain in utilizing these data, it was notable that some image sections were substantially superior to DIDSON images from 2021.

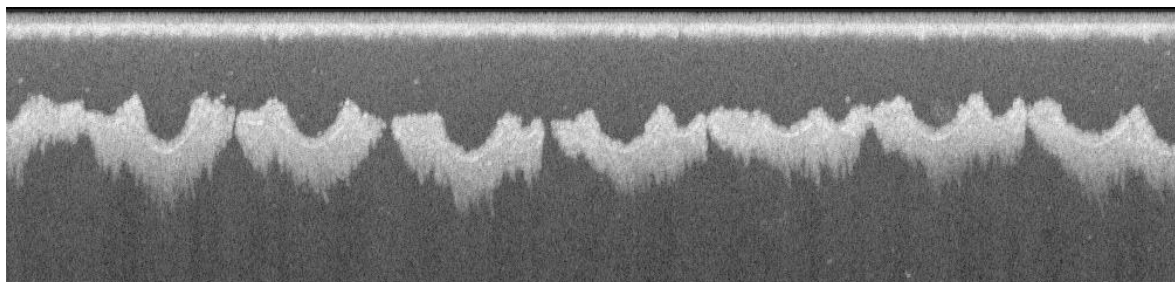


Figure 21 *Humminbird (year 2022) data example*

Figure 21 Arcs of individual seaweed line segments were visible (**Figure 21**), including the seaweed hanging off these line arcs. Seaweed individuals could not be readily identified in the image. This implies that biomass estimation will have to be performed in terms of the image area occupied by the seaweed coupled with the boat velocity. The methods outlined in the preceding section may be used towards this goal.

For the analysis of the 2022 Humminbird data, deeper networks were applied than in the previous year. This was done because more image data of seaweed were available, and so larger networks were considered before overfitting becomes a likely issue.

The data was preprocessed using the PyHum library, which allowed import of data from various Humminbird devices. As part of preprocessing, PyHum divides the input into multiple segments to facilitate further processing. The 2022 Humminbird data was divided into nine such segments, because this is more convenient for handling than a single output segment, and this also separated the highest quality data (segment 9) from the lower quality data (as described in the following).

Of these 9 segments, 6 show appreciable amounts of seaweed. However all except one of these segments show two lines overlapping (with one segment show three simultaneously). One possible the Humminbird was capturing signals reflected off neighbouring lines.

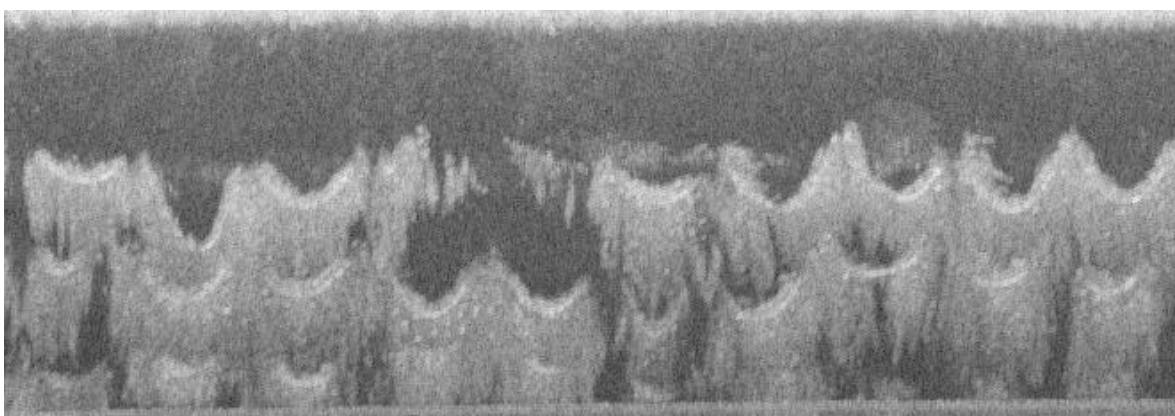


Figure 22 *Images from a segment showing 2 and 3 seaweed lines at points along the recording.*

As discussed in the study limitations, a critically important aspect of any future follow-up study would be to avoid capturing these extra lines. With these extra lines in an image, it was no longer possible to estimate the seaweed area because, some seaweed became occluded.

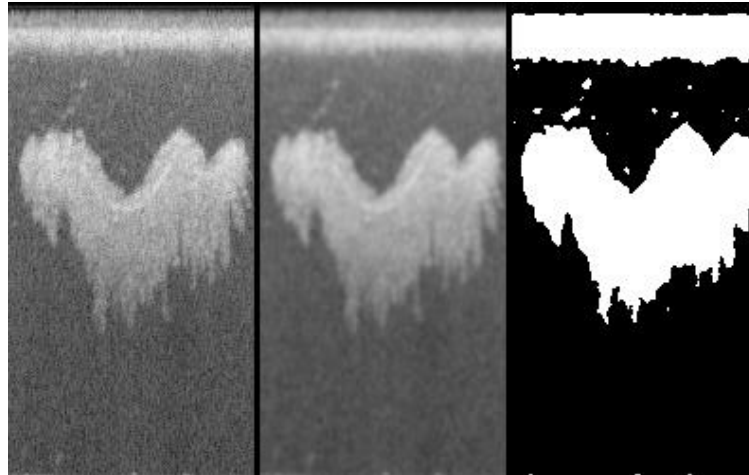


Figure 23 Demonstration of the basic segmentation process. The noisy left-most image is denoised using a Gaussian filter producing the middle image. The middle image is then thresholded to produce the mask of potential seaweed areas on the right.

However, one segment exhibited no such spurious lines, segment 9, and has been used for training and testing of new models, also in a leave-one-out manner as with the 2021 DIDSON data. The segment was partitioned into 10 parts. Out of these 10 parts, 6 show appreciable quantities of seaweed. Testing on these parts was employed to evaluate the architectures in (Fig **Figure 13** and Fig **Figure 14**.)

3.3.1 Classical Approach

Image data from segment 9 (**Figure 21**) show seaweed that is largely distinct from background in brightness, and separate from other objects and boundaries. This situation may admit simpler classical solutions to the segmentation problem. In practice, imaging conditions are rarely entirely uniform and the subjects themselves (seaweed, lines and other objects) can exhibit differences that justify a flexible approach such as using a neural network.

The rules, as described in the Materials and Methods, were developed by taking a small section of segment nine, and adjusting the procedure on it. When applied to the entire section, the result can be seen in (**Figure 24**) and (Fig **Figure 25**).



Figure 24 Result of the classical approach on segment nine. Areas marked to be ignored are tinted purple, areas considered seaweed are tinted cyan.

The procedure resulted in clean segmentation with minimal amounts of non-seaweed objects accidentally detected (for example, the pole towards the left of the segment). Close-up views (**Figure 25**) reveal that the segmentation appears to be of reasonably good quality, with details like seaweed drooping out of the main mass included.

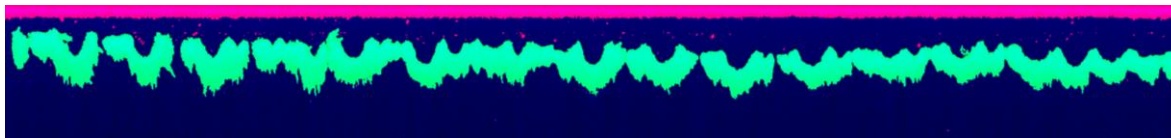


Figure 25 Closeup of the segment 9 segmentation. Areas to be ignored are coloured magenta. Cyan is used to indicate seaweed.

However, classical approaches tend to suffer from sensitivity to parameter choices (such as the threshold values). If tested on new data, such a system may fail. Consider the segmentation shown for the eight segment, the algorithm detected most of the seaweed correctly, and discarded the section of seabed on the right (**Figure 26**). Notable problems were the detection of the top region as seaweed, a short segment of seaweed as background and a false positive on the lefthand edge of the image. The detection of the top region was largely due to seaweed regions contacting this region (and so are treated as a single region).



Figure 26 Segment eight segmentation using the classical approach. Areas to be ignored are coloured magenta. Cyan is used to indicate seaweed.

These challenges illustrate the problems fixed rule systems are prone to. Simultaneously, the classical approach does perform useful, if imperfect, work. We therefore propose using neural network-based approaches to perform segmentations, but to use the classical approach to help provide ground truth segmentations for the neural networks. A human will edit these segmentations to make corrections when needed, but this is substantially less work than producing a full segmentation with such assistance. This process can be likened to using the classical approach and the human as teachers for the neural network. It is known that, in some cases, pupil networks can surpass teacher performance by learning new rules that generalize better. We discuss the results of this approach in the next section.

Before continuing, it is important to stress that, because segments one through eight do not conform to the required capture conditions we observed in segment nine, using results on these data as indicative of test performance is not recommended. Rather, new training and testing data needs to be collected in a follow-up study. That being said, we can make qualitative statements about how the systems react to these data, keeping in mind the data in these segments' limitations.

3.3.2 Neural Network Approaches

Our goal with using neural networks is to avoid manual assembly of sets of rules which become brittle when faced with new data. Towards this, the segmented images for segment nine were edited by a human annotator to correct problems in the segmentation. This then became the training data for the neural network approaches whose architectures were described in (**Figure 13**) and (Fig **Figure 14**) (hereafter referred to as Deep3 and Deep5 respectively). For training and testing, segment nine was partitioned into 10 parts and training was sequentially run on all except one part. The one remaining part was used for testing of the resulting model. Therefore, 10 different models were trained for both of Deep3 and Deep5 (this should be borne in mind when interpreting the results).

3.3.2.1 Training Procedure

The neural networks were implemented and trained using PyTorch in the Python language. Each architecture was given an initial run, and a rerun. The training loop passed through the training 100 times (100 epochs). Images were initially batched 2 at a time, but were rerun batched by 3. This was increased to make it more likely that the model will see a mixture of positive (containing seaweed) and negative (seaweed absent) images in each training step. To increase the apparent amount of data available, images were randomly flipped horizontally on during the rerun.

3.3.2.2 Qualitative Results

In this subsection, we show the resulting output for the first runs and reruns of the workflow for the Deep3 and Deep5 architectures in (Figure 27), (Fig Figure 28), (Fig Figure 29) and (Fig Figure 30). The results of the two architectures are shown side by side. The results of different runs are shown in separate figures. The first figure for each run shows the output, which the second figure highlight the errors made by the network relative to the ground truth.

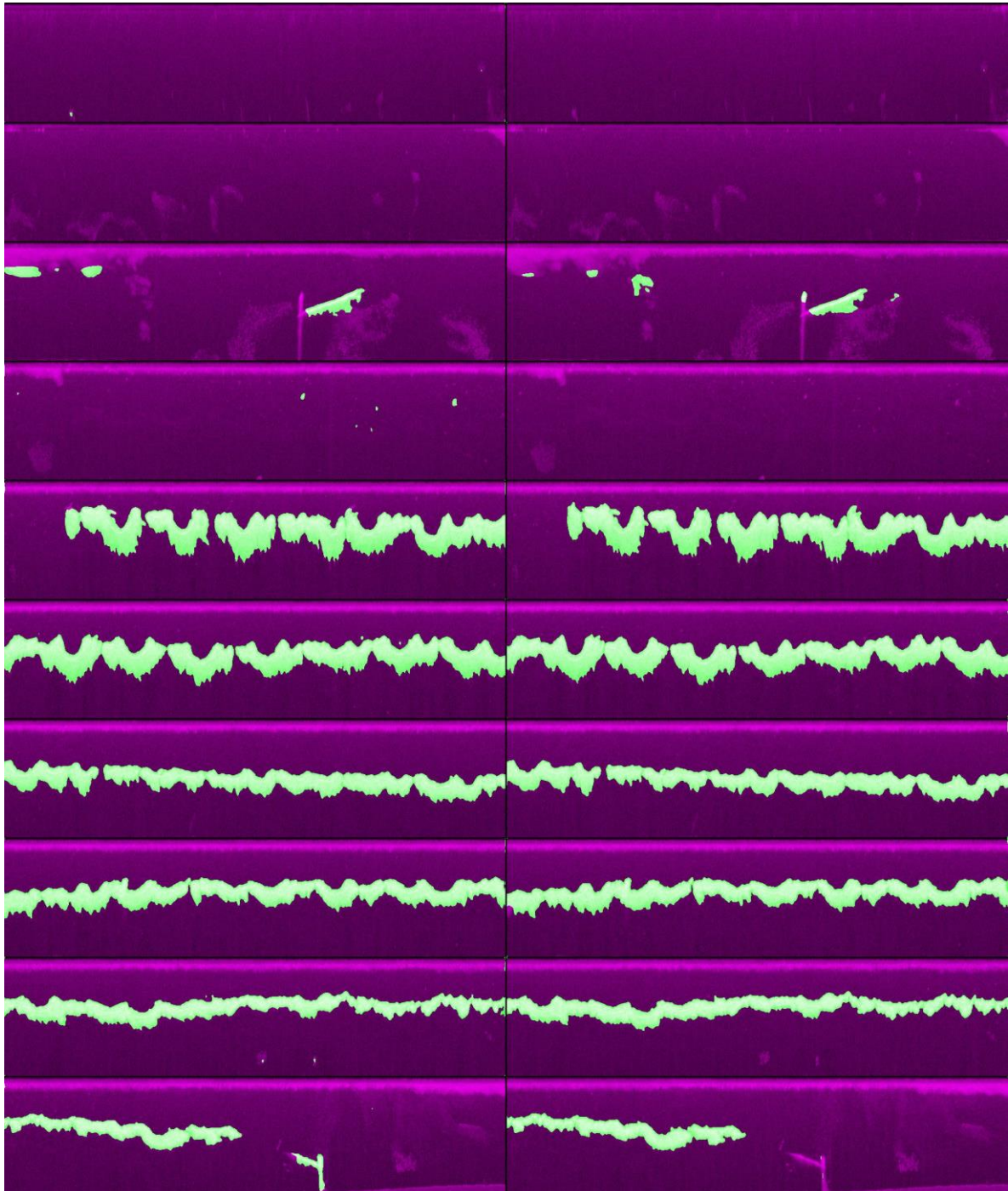


Figure 27 Neural network output superimposed on input from segment nine for Deep3 (left) and Deep5 (right) architectures after first run. Parts appear from top (1) to bottom (10). Green areas are considered seaweed by the network, areas coloured magenta are not.

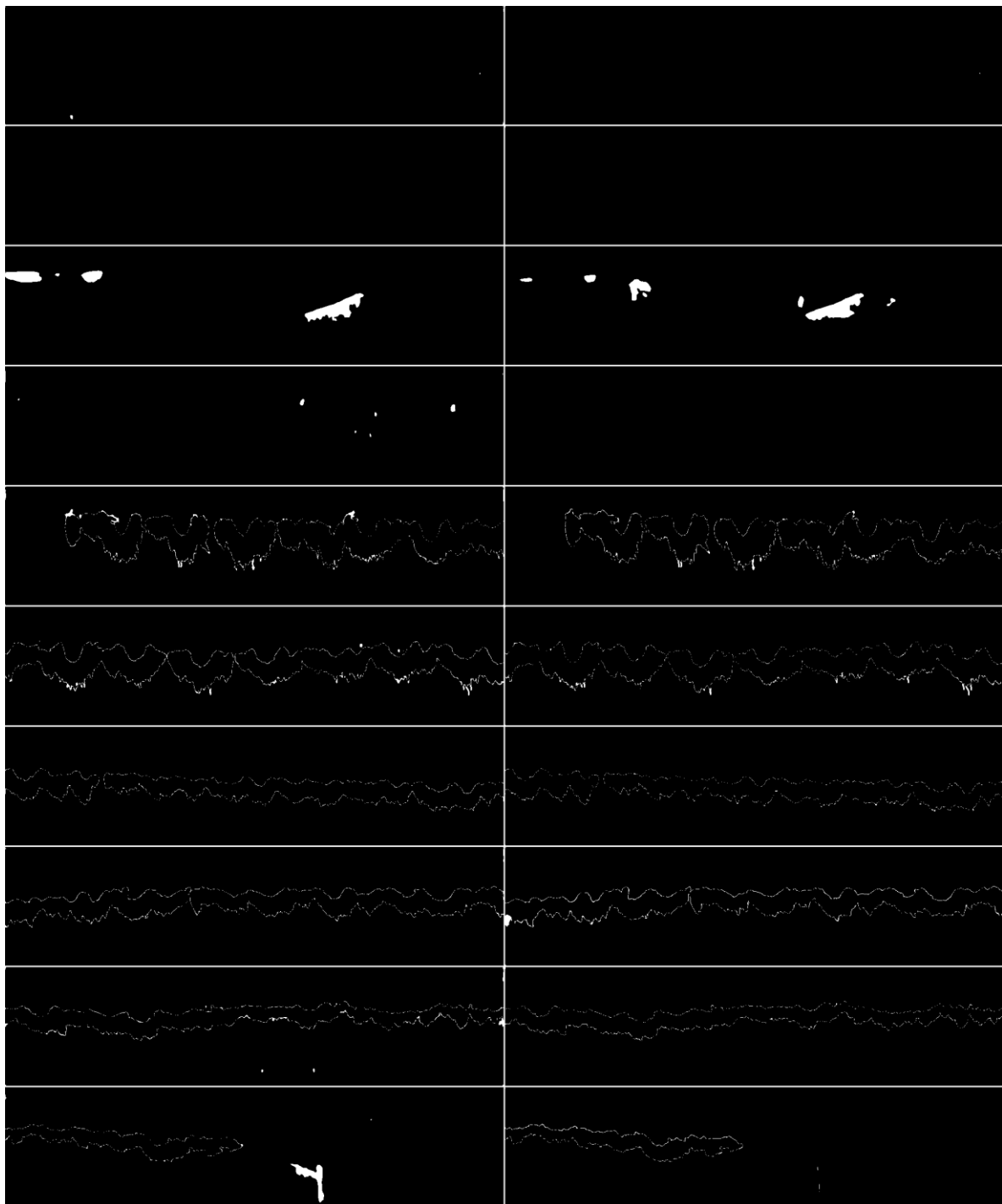


Figure 28 Neural network output error on input from segment nine for Deep3 (left) and Deep5 (right) architectures after first run. Parts appear from top (1) to bottom (10). Black regions are correct predictions, white regions are mistaken predictions.

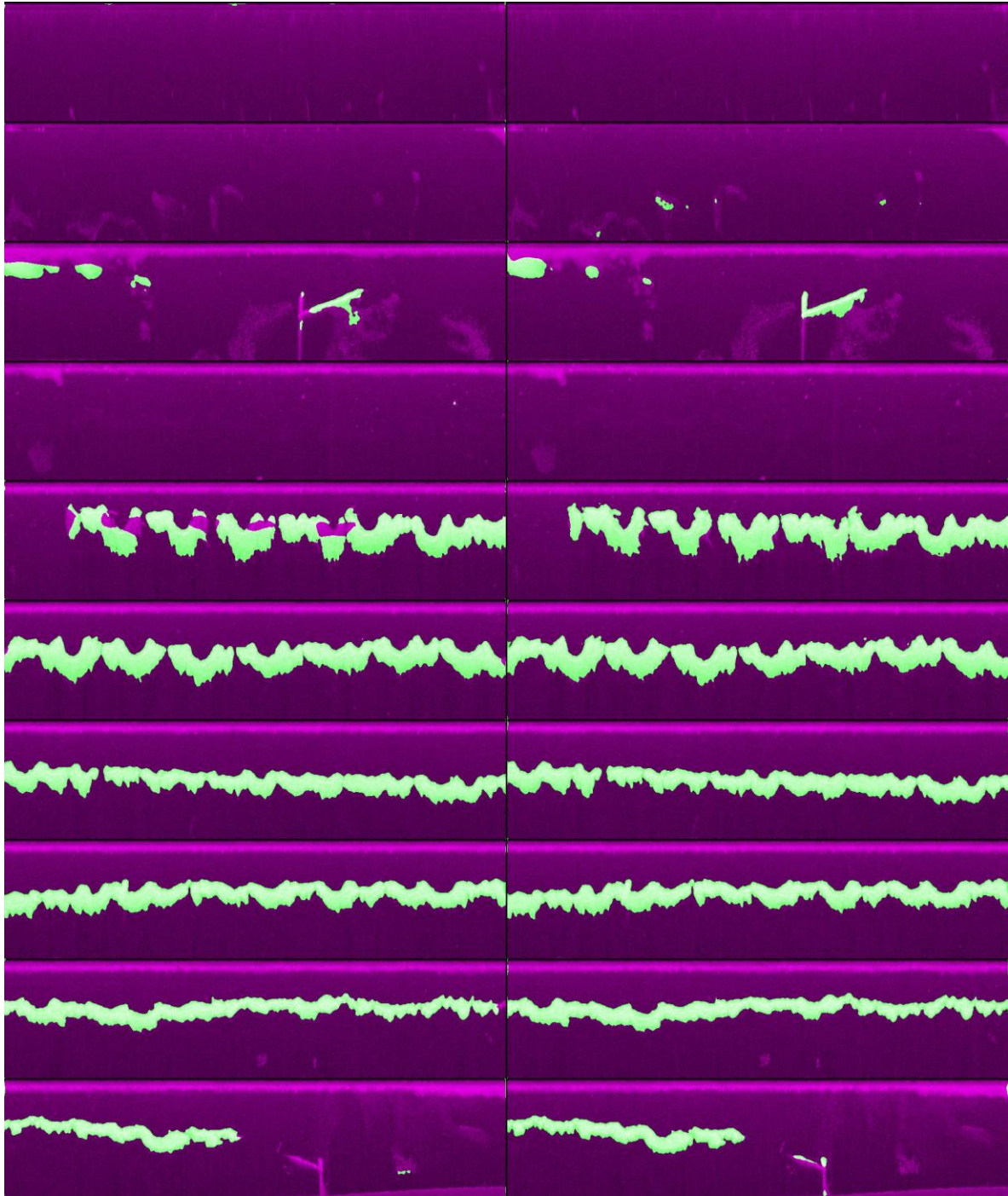


Figure 29 Neural network output superimposed on input from segment nine for Deep3 (left) and Deep5 (right) architectures after rerun. Parts appear from top (1) to bottom (10). Green areas are considered seaweed by the network, areas coloured magenta are not.

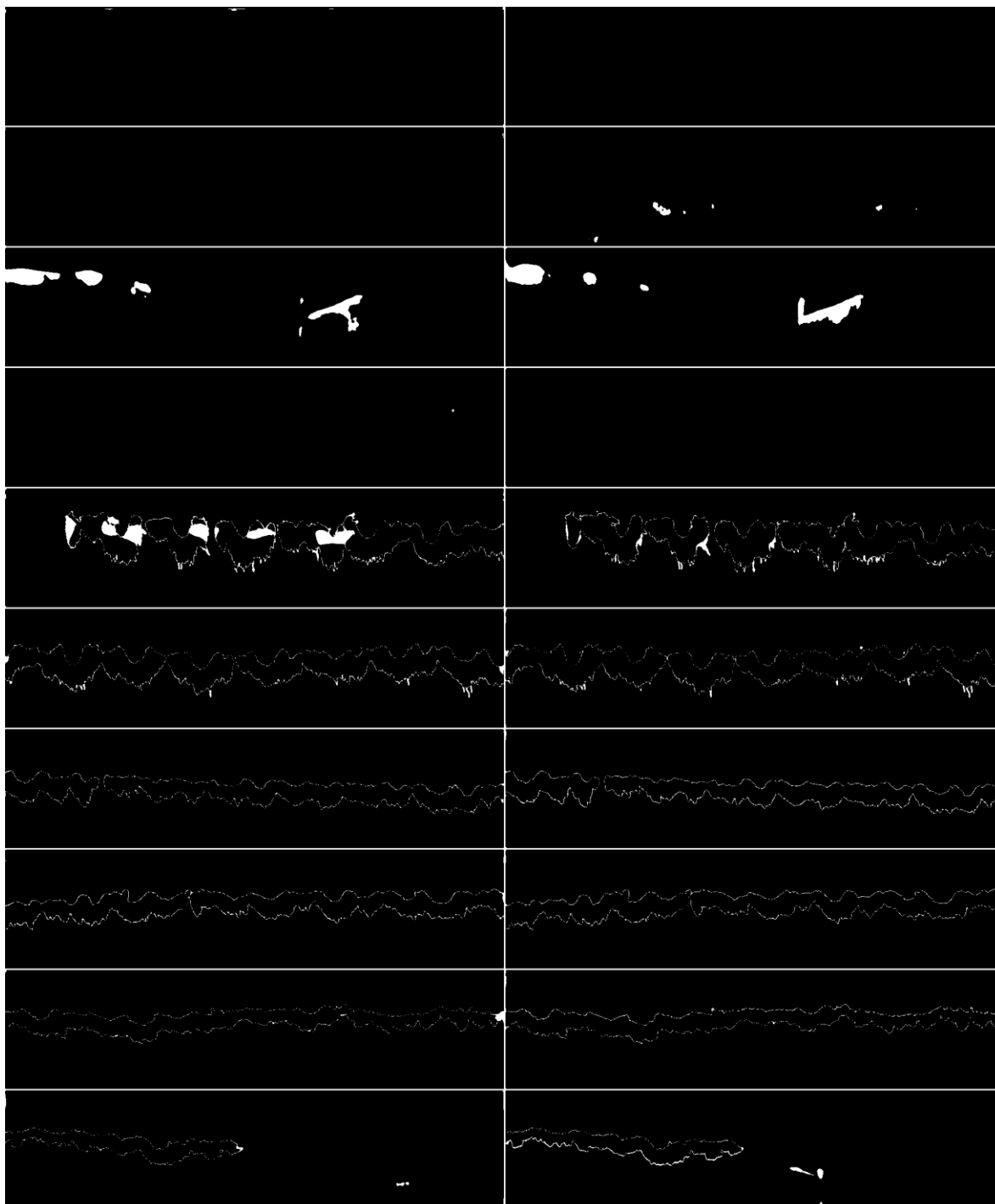


Figure 30 Neural network output error on input from segment nine for Deep3 (left) and Deep5 (right) architectures after rerun. Parts appear from top (1) to bottom (10). Black regions are correct predictions, white regions are mistaken predictions.

For the initial run, it can be noted that both architectures perform similarly. However, the Deep5 architecture performed better in certain respects. Considering the background and non-seaweed objects, the Deep3 architecture produced more false detections than the Deep5 architecture (in this run).

The quality of the rerun segmentations was, surprisingly, not as good as for the initial run. Note for example the extra errors in the part 5 segmentation of seaweed regions by Deep5. It was less clear which architecture performs best. Deep3 made notable errors in part 5 of the segment, while Deep5 appeared more likely to produce spurious small spots in the segmentation.

3.3.2.3 Quantitative Results

To evaluate system performance quantitatively, two metrics were used. One metric is the accuracy, which measures the percentage of agreement between the ground truth image and the model prediction image when they are overlaid on top of one another and corresponding positions are compared (Table 4). Areas where the ground truth and predictions differ do not increase the accuracy, as these represent mistakes. Areas where the ground truth and the predictions are the same contribute to higher accuracy, as these are correct predictions. Only results for segments five through 10 are provided because other segments did not contain appreciable seaweed.

While the lowest score in Table 4 is 96,1%, the accuracy is not necessarily the best metric to evaluate system performance. In this case, most image pixels belong to the background class, and so accuracy is skewed towards performance on background. Therefore this table is provided for reference purposes, a different metric was used instead to further discuss performance.

Table 4

Accuracies for the different runs on the architectures expressed individually for each segment, as well as pooled together for an overall accuracy.

Architecture/Run	Segment 5	Segment 6	Segment 7	Segment 8	Segment 9	Segment 10	Overall
Deep3/Initial	99,1%	99,0%	99,5%	99,3%	99,3%	99,2%	99,2%
Deep5/Initial	99,2%	99,3%	99,6%	99,0%	99,5%	99,7%	99,4%
Deep3/Rerun	96,1%	99,0%	99,4%	99,1%	99,5%	99,7%	98,8%
Deep5/Rerun	98,6%	99,1%	99,0%	99,2%	99,3%	99,2%	99,1%

The Intersection over Union (IoU) (as discussed in 2.2.8) was used to evaluate the segmentation quality with more emphasis on the foreground (Table 5).

Table 5

Intersection over Union (IoU) for the different runs on the architectures expressed individually for each segment, as well as pooled together for an overall IoU. Cases with performance lower than 90% are marked in red for convenience.

Architecture/Run	Segment 5	Segment 6	Segment 7	Segment 8	Segment 9	Segment 10	Overall
Deep3/Initial	95,3%	94,9%	96,6%	95,6%	94,8%	86,5%	94,8%
Deep5/Initial	96,2%	96,5%	97,1%	94,1%	96,3%	94,3%	95,9%
Deep3/Rerun	81,1%	94,9%	95,8%	94,3%	95,7%	94,5%	91,9%
Deep5/Rerun	93,0%	95,5%	93,8%	94,8%	94,9%	87,6%	93,9%

The IOU values support the earlier qualitative discussion around the performance of the different approaches. In both runs, Deep5 outperforms Deep3 (Table 4). It is notable that the rerun performance is worse in both case.

Three values were below 90% (Table 5, bolded in red). For the initial run, Deep3 attains 86.5% for part 10. This was caused by detecting a large non-seaweed object as seaweed (**Figure 28**) (Deep5 avoids this). In the rerun, Deep5 made a mistake (**Figure 30**), although here the thickening of the boundary around the seaweed region may play some role. Deep3 made the worst seaweed segmentation errors of the two runs.

The reported IOU values and qualitative plots indicate that the architectures were generally successful at identifying seaweed. In addition, we can see the top region and seabed are correctly ignored by the

detectors. In certain cases, non-seaweed objects are still detected. However, this is not unsurprising, as non-seaweed object is a very broad category. The models may need more data to learn this distinction more reliably.

Note also in (**Figure 28**) and (Fig **Figure 30**) that the ends of some seaweed individuals were not correctly detected. This could be due to how the ground truth is generated. Most pixels were annotated using the classical method, while the minority were annotated by a human. The neural network may find it easier to learn the classical method's annotations, and is rewarded for this because most pixels are annotated with this method. To address this, future studies should attempt to weight the human annotations more strongly so that the models have an incentive to learn them. More training data can also help, as it would allow the models the better spot regularities in human annotations.

3.3.2.4 Application to other segments

Up to this point, the analysis has not considered performance on the other segments (1 through 8). This is because the quality of these segments is not enough to represent a fair test. Nevertheless, it may be instructive to plot the segmentation of these recording segments. This is shown in (**Figure 31**). Here we employed the model from the initial run of Deep5 testing on part 6. This keeps data from the larger (part 5) and smaller (parts 7 through 10) seaweed regions available.

Examination of these results suggests at least three conclusions:

1. Seaweed regions are largely detected, although regions close to the top or the seabed tend to be dropped. This may be corrected either by including sufficient training data where the seaweed is at one of these extremes (assuming segmentation is still possible in such a situation), or the physical handling of the sensor may be changed.
2. The top region and the seabed remain largely (correctly) undetected. Note that for some other models, this was not the case. Here too, additional data may help.
3. The handling of non-seaweed objects is mixed. Some are correctly undetected, but mistakes do occur as well. Non-seaweed objects are quite variable, and more examples are needed to help the network learn the distinction between these objects and seaweed.

3.3.3 Summary and conclusion

In this subsection, we have discussed a classical approach for segmenting the 2022 Humminbird data. The classical approach was successful on segment 9, but could be expected to be less flexible when obtaining new data. Instead, this approach was used to facilitate the labelling of the data for use by a set of neural network-based approaches. Such systems, when provided with sufficient data, are known to be more robust to natural variation within input data (as long as this was reflected in the training data). The systems were shown to be successful during a leave-one-out evaluation on segment 9 (one system achieving 95.9% IoU overall). These results suggest that a combination of the Humminbird with neural network-based approaches show promise if the problem of "extra" lines can be solved, and enough data are gathered for making the models more robust to natural variation.

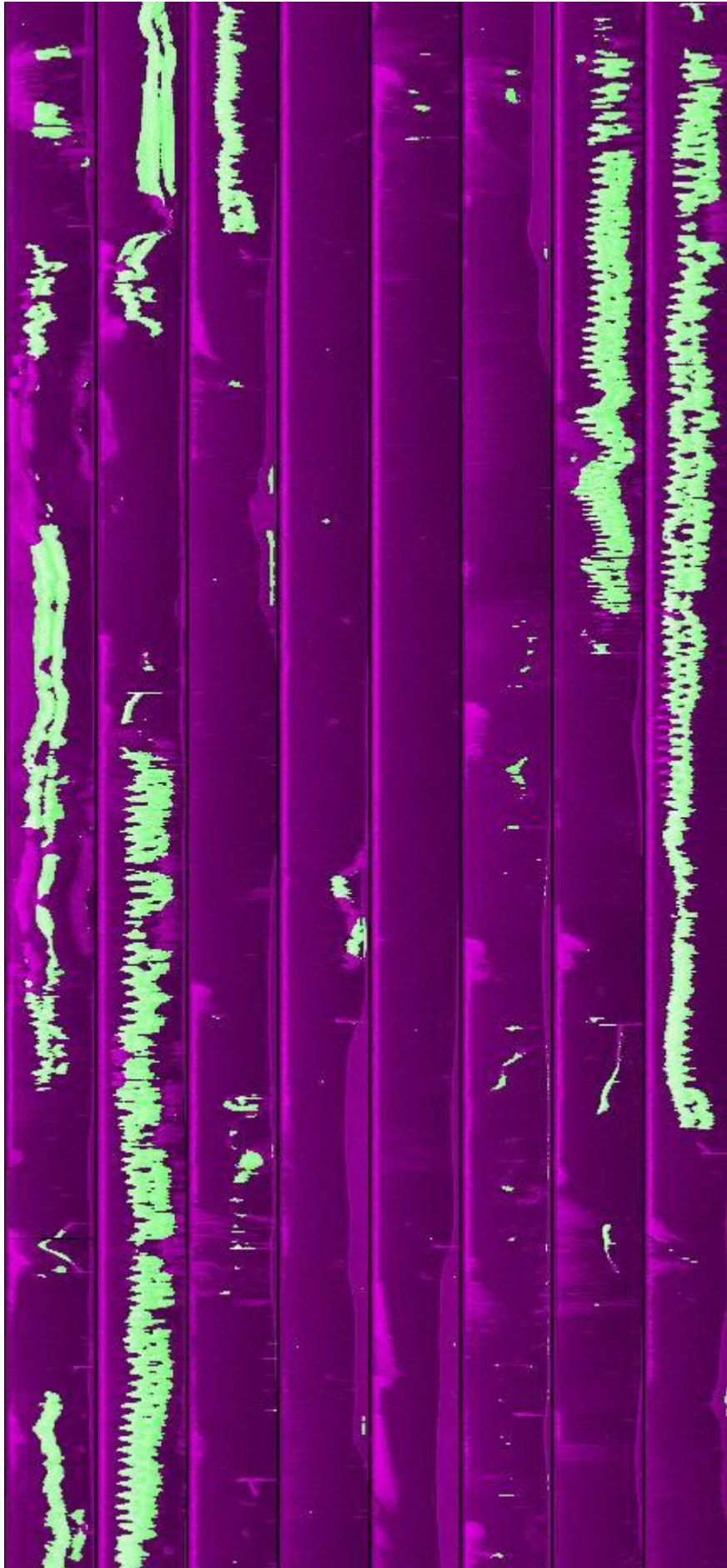


Figure 31 Segmentations of other segments using model from part 6 of segment 9. Architecture is Deep5 from initial run (best performing case). Segments are numbered 1 through 8 from left to right.

3.4 Seaweed biomass

The sampled length of rope with *S. latissima* was 21 meters long. The total weight of the rope during the first measurement was 31,7 kg, as comparison we also weighed a piece of rope of the same length which was not seeded with seaweed. This rope weighted 4.6 kg, therefore the weight of the seaweed during the first measurement was 27,1 kg (Table 6.).

During the second measurement the seaweed had grown so much it had to be placed in two fish boxes without cutting the line, the boxes were weighted individually and added up, after which the weight of the boxes was subtracted.

Table 6 Seaweed biomass

Date	Length of rope	Weight of Seeded rope	Weigh of empty rope	Seaweed biomass
31-03-2021	21 meter	31.7 kg	4.6 kg	27.1 kg
01-06-2021	21 meter	110.5 kg	4.6 kg	105.9 kg

In addition to the weight, a smaller piece of rope was cut off on the harvesting day, for a more detailed look. This approximately 15 cm piece of cultivation line, on this piece of line each seaweed piece was counted and photographed so exact surface area (SA) could be calculated using a binary image in the programme ImageJ. Additionally 10 of the largest pieces of seaweed were weighted for fresh weight and dry weight. The 15 cm rope segment contained in total 84 individual seaweed pieces. With a combined wet weight of 710 gr (excluding rope) the 84 seaweed blades had a total surface area of 1,751 m². The largest piece of seaweed measured 83.6 cm in length and had a SA of 1059 cm² while the blade with the largest SA, 1589.3 cm², had a total length of 83.6 cm. All length and SA's were calculated excluding the holdfast. To see if there was a correlation between the weight and the length or SA of the seaweed a simple regression line was made and R² was determined using only the 10 largest pieces of seaweed (Fig 32.).

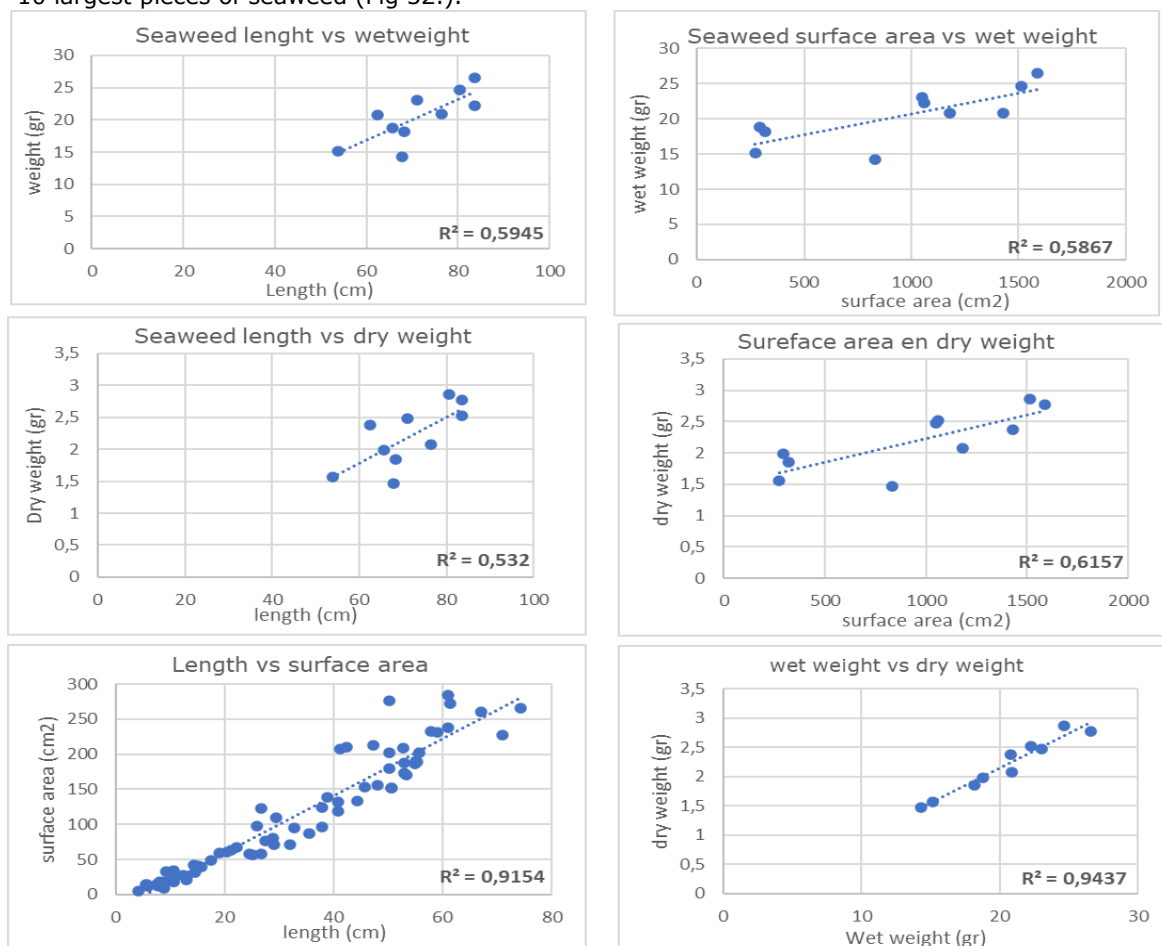


Figure 32. regression graphs of the seaweed length, surface area, dry weight and wet weight. correlations were only found in the bottom two graphs.

However no correlation was found, except for the combination, wet weight vs dry weight ($R^2 = 0.9437$), however this is a known correlation. Where the dry/wet ratio for *S. latissima* is approximately 0.12, though this ratio does vary a bit per location and season (Broch and Slagstad, 2012; Campbell et al., 2019). What was interesting was that the length and surface area did have a correlation when only the 74 remaining (smaller) seaweed blades were taken into account ($R^2 = 0.9154$). This means that if you want to determine an equation for biomass of seaweed based on length or the SA, you might need a different equation for the smaller seaweed pieces than for the larger ones.

4 Conclusions and recommendations

4.1 Limitations

While the study yielded promising results with respect to seaweed segmentation from sonar images (especially with the Humminbird sensor), certain key limitations remain that need to be addressed by any follow-up study.

- Sonar recording procedure is not yet optimized for reliable good quality image capture. It is also not clear yet whether improving the sensor handling can lead to enough improvement in the image quality in the setting of a typical seaweed farm. In particular, the “extra” lines should be eliminated from images, and it must still be determined whether this is possible. Also important is that the images should be capturable in a repeatable way, there should be a handling procedure for the sonar which leads to usable data recording.
- The dataset size was limited by the needs of deep learning architectures (though architectures with generally lower data requirements were used in these experiments). This meant analysis was limited to a demonstration of candidate neural network architectures using leave-one-out cross validation. Models trained on limited data are unlikely to generalize well to data captured in a new setting, however these results did show the models (referring to the case of the Humminbird data) can be successfully applied to data captured within the same recording run.

While measuring the area of the seaweed regions based on segmented appears likely to be related to biomass measurements, the extent of such a correlation needs to be determined, and actual biomass predictions need to be made using the segmentations. This implies that sufficient biomass measurements need to be made for training and testing models.

4.2 Feasibility

From the 2022 data, the feasibility in using the Humminbird sonar for the estimation of seaweed biomass in a cultivation setting is promising, subject to further feasibility explorations around the proper capture procedure within a seaweed farm context. The 2022 results of the field surveys showed that the Humminbird sonar could detect seaweed, and that it was superior to the DIDSON. The 2021 results showed mussel cultivation lines which hung on either side of the seaweed line, which may be useful in applications dealing with mussels. While the DIDSON did show seaweed in some images, its feasibility is reduced by the difficulty of handling the device, as well as what appears to be more difficulty capturing usable seaweed images. Furthermore, the DIDSON is not a cheap device, nor an easy to use piece of equipment. Interpretation of the images was also more difficult.

The use of a convolutional network model to recognise seaweed images and estimate the biomass appears promising. During this study it was found that the limited number of usable images to train the machine learning model was severely limiting the results of the model in the case of the DIDSON analysis, and less severely in the case of the Humminbird sonar. Nonetheless, promising results were acquired and with the now ready to use code the model can easily be improved by adding more images, if the aforementioned limitations are addressed. This feasibility studies as next steps: (1) determination of whether the “extra lines” and other artifacts can be removed (2) establish a repeatable procedure for measuring with the Humminbird sonar (3) increase the dataset size designing for deep learning experiments (4) addition of biomass measurements to train and test the estimation of biomass. To the this more seaweed lines need to be sampled both with a sonar technique and actual biomass measurements to train the model (the scope of this should also be designed with deep learning experiments in mind).

4.3 Applicability

The Humminbird sonar seems applicable in detecting seaweed (given the 2022 data). In addition, on the 2021 images the mussel cultivation lines were clearly visible and in the future studies could be used to estimate mussel biomass on rope cultivation. Further research needs to be done to explore this possibility. The DIDSON showed some promise, but ultimately the Humminbird sonar appeared more applicable.

4.4 Recommendations

The present study established that using the Humminbird sonar for seaweed detection may be feasible. In this section we relate the recommended steps towards biomass estimation through sonar for seaweed cultivation applications.

1. To confirm that the Humminbird sonar is suitable, a follow-up study must test whether the empty captures and “extra lines” seen in some of the recording segments can be eliminated within a real seaweed cultivation setting. This study must also establish a recording procedure that can reliably be used to record high quality images of seaweed. This study ends in a go/no-go decision.
2. Given the success of the preceding study, a further experiment must test the usability of the deep learning methods for estimating seaweed biomass. Thus far, we have shown potential for segmentation without connecting to biomass prediction. This requires (1) a large enough dataset of seaweed images for training and testing deep learning models so that models may be reused in similar settings (2) corresponding measurements of seaweed biomass. It is important to emphasise that fine-grained seaweed biomass measurements will be necessary to strengthen the analysis (this may require temporary changes to farming / measurement practice to enable such measurements to be taken).
3. Ground truth was partially obtained using an automatic procedure including (as one component) convolution, the rest by human annotation. Ground truth from the automatic procedure is likely more readily incorporated by the deep neural networks (which are convolutional networks). It would be informative in future studies to separate performance on labels provided by the automatic procedure and humans. If necessary, the models can be guided to incorporating human annotations by weighting such annotations more highly in the cost function being optimized during the training procedure.

5 Quality Assurance

Wageningen Marine Research utilises an ISO 9001:2015 certified quality management system. The organisation has been certified since 27 February 2001. The certification was issued by DNV.

References

- Apple Inc. (2016, September), vImage Programming Guide: Performing Convolution Operations. Retrieved from <https://developer.apple.com/library/archive/documentation/Performance/Conceptual/vImage/ConvolutionOperations/ConvolutionOperations.html>
- Azevedo, C.I., Duarte, M.P., Marinho, S.G., Neumann, F., Sousa-Pinto, I., 2019. Growth of *Saccharina latissima* (Laminariales, Phaeophyceae) cultivated offshore under exposed conditions, *Phycologia*, 58, 5, Special issue on seaweed aquaculture, P 504-515, DOI: [10.1080/00318884.2019.1625610](https://doi.org/10.1080/00318884.2019.1625610)
- Campbell, I., Macleod, A., Sahlmann, C., Neves, L., Funderud, J., Øverland, M., Hughes, A.D. and Stanley, M. 2019. The Environmental Risks Associated With the Development of Seaweed Farming in Europe - Prioritizing Key Knowledge Gaps. *Frontiers in Marine Science* 6.
- Bennion, M., Yesson, C., Brodie, J. (2017) Remote sensing of kelp: novel methods for mapping and monitoring wild kelp resources. A report for The Crown Estate. (PDF)
- Bennion, M. (2018) What is the best way to monitor kelp? The fun/efficiency trade-off. Macroalgal research group.
- Bennion, M., Fisher, J., Yesson, C., Brodie, J. (2019) Remote sensing of kelp (Laminariales, Ochrophyta): monitoring tools and 2 implications for wild harvesting, *Reviews in Fisheries Science & Aquaculture*, 27:2, 127-141, DOI: [10.1080/23308249.2018.1509056](https://doi.org/10.1080/23308249.2018.1509056)
- Broch, O.J. and Slagstad, D. 2012. Modelling seasonal growth and composition of the kelp *Saccharina latissima*. *Journal of applied phycology* 24(4), 759-776.
- Lubsch, A., Burggraaf, D., & Lansbergen, R. (Ed.) (2020). *Feasibility study on remote estimation of biomass in a seaweed cultivation farm applying sonar : technical report*. (Wageningen Marine Research rapport; No. C110/20). Wageningen Marine Research. <https://doi.org/10.18174/536545>
- Shanmugamani, R. 2018. [Deep Learning for Computer Vision](#). Packt Publishing.
- Ronneberger, O., Fischer, P., & Brox, T. (2015). U-net: Convolutional networks for biomedical image segmentation. In *Proceedings of the International Conference on Medical Image Computing and Computer-Assisted Intervention* (pp. 234-241). Springer, Cham. https://doi.org/10.1007/978-3-319-24574-4_28

Justification

Report C010/23

Project Number: 4318300156

The scientific quality of this report has been peer reviewed by a colleague scientist and a member of the Management Team of Wageningen Marine Research

Approved: Olvin van Keeken
Researcher

Signature:



4 March 2023

Date:

Approved: Dr. Ir. T.P. Bult
Director

Signature:



4 March 2023

Date:

Wageningen Marine Research
T +31 (0)317 48 7000
E: marine-research@wur.nl
www.wur.eu/marine-research

Visitors' address

- Ankerpark 27 1781 AG Den Helder
- Korringaweg 7, 4401 NT Yerseke
- Haringkade 1, 1976 CP IJmuiden

With knowledge, independent scientific research and advice, **Wageningen Marine Research** substantially contributes to more sustainable and more careful management, use and protection of natural riches in marine, coastal and freshwater areas.



Wageningen Marine Research is part of Wageningen University & Research. Wageningen University & Research is the collaboration between Wageningen University and the Wageningen Research Foundation and its mission is: 'To explore the potential for improving the quality of life'
